We are IntechOpen, the world's leading publisher of Open Access books Built by scientists, for scientists

4,800
Open access books available

122,000
International authors and editors

135M
Downloads

Our authors are among the

154
Countries delivered to

TOP 1%
most cited scientists

12.2%
Contributors from top 500 universities

CLARIVATE ANALYTICS BOOK CITATION INDEX INDEXED

WEB OF SCIENCE™

Selection of our books indexed in the Book Citation Index in Web of Science™ Core Collection (BKCI)

Interested in publishing with us?
Contact book.department@intechopen.com

Numbers displayed above are based on latest data collected.
For more information visit www.intechopen.com

20

Heat Transfer in Nanostructures Using the Fractal Approximation of Motion

Maricel Agop[1,2], Irinel Casian Botez[3],
Luciu Razvan Silviu[4] and Manuela Girtu[5]
[1]*Laboratoire de Physique des Lasers, Atomes et Molécules (UMR 8523), Université des Sciences et Technologies de Lille,*
[2]*Physics Department, "Ghe. Asachi" Technical University, Iasi,*
[3]*Department of Electronics, Telecommunication and Information Technology, "Gh. Asachi" Technical University, Iasi,*
[4]*Faculty of Civil Engineering, "Ghe. Asachi" Technical University, Iasi,*
[5]*"Vasile Alecsandri" University of Bacau, Department of Mathematics, Bacau*
[1]*France*
[2,3,4,5]*Romania*

1. Introduction

If at a macroscopic scale the heat transfer mechanism implies either diffusion type conduction or phononic type conduction (Zhang, 2007; Rohsenow et al., 1998), at a microscopic scale the situation is completely different. This happens because the macroscopic familiar concepts cannot be applied at a microscopic scale, e.g. the concept of a distribution function of both coordinates and momentum used in the Boltzmann equation (Wang et al., 2008). Moreover, fundamental concepts such a temperature cannot be defined in the conventional sense, *i.e.* as a measure of thermodynamic equilibrium (Chen, 2000). Thus anomalies might occur: the thermal anomaly of the nanofluids (Wang&Xu, 1999; Keblinski et al., 2002; Patel et al., 2003), etc.

According to our opinion, anomalies become normalities if their specific measures depend on scales: heat conduction in nanostructures differs significantly from that in macrostructures because the characteristic length scales associated with heat carriers, *i.e.* the mean free path and the wavelength, are comparable to the characteristic length of nanostructures (Chen, 2000). Therefore, we expect to replace the usual mechanisms (ballistic thermal transport, etc.) by something more fundamental: a unique mechanism in which the physical measures should depend not only on spatial coordinates and time, but also on scales. This new way will be possible through the Scale Relativity (SR) theory (Notalle, 1992, 2008a, 2008b, 2007). Some applications of the SR theory at the nanoscale was given in (Casian Botez et al., 2010; Agop et al. 2008). In the present paper, a new model of the heat transfer on nanostructures, considering that the heat flow paths take place on continuous but non-differentiable curves, i.e. an fractals, is established.

2. Consequences of non-differentiability in the heat transfer processes

Let us suppose that the heat flow take place on continuous but non-differentiable curves (fractal curves). The non-differentiability implies the followings (Notalle, 1992, 2008a, 2008b, 2007):

i. A continuous and a non-differentiable curve (or almost nowhere differentiable) is explicitly scale dependent, and its length tends to infinity, when the scale interval tends to zero. In other words, a continuous and non-differentiable space is fractal, in the general meaning given by Mandelbrot to this concept (Mandelbrot, 1982);

ii. There is an infinity of fractals curves (geodesics) relating any couple of its points (or starting from any point), and this is valid for all scales;

iii. The breaking of local differential time reflection invariance. The time-derivative of the temperature field T can be written two-fold:

$$\frac{dT}{dt} = \lim_{dt\to 0} \frac{T(t+dt) - T(t)}{dt}$$
$$\frac{dT}{dt} = \lim_{dt\to 0} \frac{T(t) - T(t-dt)}{dt} \qquad (1a,b)$$

Both definitions are equivalent in the differentiable case. In the non-differentiable situation these definitions fail, since the limits are no longer defined. In the framework of fractal theory, the physics is related to the behavior of the function during the "zoom" operation on the time resolution δt, here identified with the differential element dt ("substitution principle"), which is considered as an independent variable. The standard temperature field $T(t)$ is therefore replaced by a fractal temperature field $T(t,dt)$, explicitly dependent on the time resolution interval, whose derivative is undefined only at the unobservable limit $dt \to 0$. As a consequence, this lead us to define the two derivatives of the fractal temperature field as explicit functions of the two variables t and dt,

$$\frac{d_+T}{dt} = \lim_{dt\to 0_+} \frac{T(t+dt,dt) - T(t,dt)}{dt}$$
$$\frac{d_-T}{dt} = \lim_{dt\to 0_-} \frac{T(t,dt) - T(t-dt,dt)}{dt} \qquad (2a,b)$$

The sign, +, corresponds to the forward process and, -, to the backward process;

iv. the differential of the fractal coordinates, $d_\pm X(t,dt)$, can be decomposed as follows:

$$d_\pm X(t,dt) = d_\pm x(t) + d_\pm \xi(t,dt) \qquad (3a,b)$$

where $d_\pm x(t)$ is the "classical part" and $d_\pm \xi(t,dt)$ is the "fractal part".

v. the differential of the "fractal part" of $d_\pm X$ satisfies the relation (the fractal equation)

$$d_\pm \xi^i = \lambda_\pm^i (dt)^{1/D_F} \qquad (4a,b)$$

where $\lambda_\pm^i$ are some constant coefficients, and D_F is a constant fractal dimension. We note that for the fractal dimension we can use any definition (Kolmogorov, Hausdorff

(Notalle, 1992, 2008a, 2008b, 2007; Casian Botez et al., 2010; Agop et al. 2008; Mandelbrot, 1982), etc.);

vi. the local differential time reflection invariance is recovered by combining the two derivatives, d_+/dt and d_-/dt, in the complex operator:

$$\frac{\hat{d}}{dt}=\frac{1}{2}\left(\frac{d_+ + d_-}{dt}\right)-\frac{i}{2}\left(\frac{d_+ - d_-}{dt}\right) \tag{5}$$

Applying this operator to the "position vector" yields a complex speed

$$\hat{V}=\frac{\hat{d}\boldsymbol{X}}{dt}=\frac{1}{2}\left(\frac{d_+\boldsymbol{X}+d_-\boldsymbol{X}}{dt}\right)-\frac{i}{2}\left(\frac{d_+\boldsymbol{X}-d_-\boldsymbol{X}}{dt}\right)=\frac{\boldsymbol{V}_+ + \boldsymbol{V}_-}{2}-i\frac{\boldsymbol{V}_+ - \boldsymbol{V}_-}{2}=\boldsymbol{V}-i\boldsymbol{U} \tag{6}$$

with

$$\begin{aligned}\boldsymbol{V}&=\frac{\boldsymbol{V}_+ + \boldsymbol{V}_-}{2}\\ \boldsymbol{U}&=\frac{\boldsymbol{V}_+ - \boldsymbol{V}_-}{2}\end{aligned} \tag{7a,b}$$

The real part, $\boldsymbol{V}$, of the complex speed, $\hat{\boldsymbol{V}}$, represents the standard classical speed, which is differentiable and independent of resolution, while the imaginary part, $\boldsymbol{U}$, is a new quantity arising from fractality, which is non-differentiable and resolution-dependent;

vii. the average values of the quantities must be considered in the sense of a generalized statistical fluid like description. Particularly, the average of $d_\pm\mathbf{X}$ is

$$\langle d_\pm\mathbf{X}\rangle = d_\pm\mathbf{x} \tag{8a,b}$$

with

$$\langle d_\pm\xi\rangle = 0 \tag{9a,b}$$

viii. in such an interpretation, the "particles" are indentified with the geodesics themselves. As a consequence, any measurement is interpreted as a sorting out (or selection) of the geodesics by the measuring devices.

3. Covariant total derivative in the heat transfer processes

Let us now assume that the curves describing the heat flow (continuous but non-differentiable) is immersed in a 3-dimensional space, and that $\mathbf{X}$ of components $X^i\left(i=\overline{1,3}\right)$ is the position vector of a point on the curve. Let us also consider the fractal temperature fluid $T(\mathbf{X},t)$, and expand its total differential up to the third order:

$$d_\pm T=\frac{\partial T}{\partial t}dt+\nabla T\cdot d_\pm\boldsymbol{X}+\frac{1}{2}\frac{\partial^2 T}{\partial X^i\partial X^j}d_\pm X^i d_\pm X^j+\frac{1}{6}\frac{\partial^3 T}{\partial X^i\partial X^j\partial X^k}d_\pm X^i d_\pm X^j d_\pm X^k \tag{10a,b}$$

where only the first three terms were used in the Nottale's theory (*i.e.* second order terms in the equation of motion). The relations (10a,b) are valid in any point of the space manifold

and also for the points $\boldsymbol{X}$ on the fractal curve which we have selected in relations (10a,b). From here, the forward and backward average values of this relation take the form:

$$\begin{aligned}\left\langle d_{\pm}T\right\rangle = \left\langle \frac{\partial T}{\partial t}dt\right\rangle + \left\langle \nabla T\cdot d_{\pm}\boldsymbol{X}\right\rangle + \frac{1}{2}\left\langle \frac{\partial^2 T}{\partial X^i \partial X^j}d_{\pm}X^i d_{\pm}X^j\right\rangle + \\ + \frac{1}{6}\left\langle \frac{\partial^3 T}{\partial X^i \partial X^j \partial X^k}d_{\pm}X^i d_{\pm}X^j d_{\pm}X^k\right\rangle\end{aligned} \tag{11a,b}$$

We make the following stipulation: the mean value of the function f and its derivatives coincide with themselves, and the differentials $d_{\pm}X^i$ and dt are independent, therefore the average of their products coincide with the product of averages. Thus, the equations (11a,b) become:

$$d_{\pm}T = \frac{\partial T}{\partial t}dt + \nabla T\cdot\left\langle d_{\pm}\boldsymbol{X}\right\rangle + \frac{1}{2}\frac{\partial^2 T}{\partial X^i \partial X^j}\left\langle d_{\pm}X^i d_{\pm}X^j\right\rangle + \frac{1}{6}\frac{\partial^3 T}{\partial X^i \partial X^j \partial X^k}\left\langle d_{\pm}X^i d_{\pm}X^j d_{\pm}X^k\right\rangle \tag{12a,b}$$

or more, using equations (3a,b) with the property (9a,b),

$$\begin{aligned}d_{\pm}T = \frac{\partial T}{\partial t}dt + \nabla T\cdot d_{\pm}\boldsymbol{x} + \frac{1}{2}\frac{\partial^2 T}{\partial X^i \partial X^j}\left(d_{\pm}x^i d_{\pm}x^j\left\langle d_{\pm}\xi^i d_{\pm}\xi^j\right\rangle\right) + \\ + \frac{1}{6}\frac{\partial^3 T}{\partial X^i \partial X^j \partial X^k}\left(d_{\pm}x^i d_{\pm}x^j d_{\pm}x^k\left\langle d_{\pm}\xi^i d_{\pm}\xi^j d_{\pm}\xi^k\right\rangle\right)\end{aligned} \tag{13a,b}$$

Even the average value of the fractal coordinate, $d_{\pm}\xi^i$ is null (see (9a,b)), for the higher order of the fractal coordinate average the situation can be different. First, let us focus on the mean $\left\langle d_{\pm}\xi^i d_{\pm}\xi^j\right\rangle$. If $i\neq j$, this average is zero due the independence of $d_{\pm}\xi^i$ and $d_{\pm}\xi^j$. So, using (4a,b), we can write:

$$\left\langle d_{\pm}\xi^i d_{\pm}\xi^j\right\rangle = \lambda_{\pm}^i\lambda_{\pm}^j\left(dt\right)^{(2/D_F)-1}dt \tag{14a,b}$$

Then, let us consider the mean $\left\langle d_{+}\xi^i d_{+}\xi^j d_{\pm}\xi^k\right\rangle$. If $i\neq j\neq k$, this average is zero due the independence of $d_{\pm}\xi^i$ on $d_{\pm}\xi^j$ and $d_{\pm}\xi^k$. Now, using equations (4a,b), we can write:

$$\left\langle d_{\pm}\xi^i d_{\pm}\xi^j d_{\pm}\xi^k\right\rangle = \lambda_{\pm}^i\lambda_{\pm}^j\lambda_{\pm}^k\left(dt\right)^{(3/D_F)-1}dt \tag{15a,b}$$

Then, equations (13a,b) may be written under the form:

$$\begin{aligned}d_{\pm}T = \frac{\partial T}{\partial t}dt + d_{\pm}\boldsymbol{x}\cdot\nabla T + \frac{1}{2}\frac{\partial^2 T}{\partial X^i \partial X^j}d_{\pm}x^i d_{\pm}x^j + \\ + \frac{1}{2}\frac{\partial^2 T}{\partial X^i \partial X^j}\lambda_{\pm}^{\ i}\lambda_{\pm}^{\ j}\left(dt\right)^{(2/D_F)-1}dt + \\ + \frac{1}{6}\frac{\partial^3 T}{\partial X^i \partial X^j \partial X^k}d_{\pm}x^i d_{\pm}x^j d_{\pm}x^k + \\ + \frac{1}{6}\frac{\partial^3 T}{\partial X^i \partial X^j \partial X^k}\lambda_{\pm}^{\ i}\lambda_{\pm}^{\ j}\lambda_{\pm}^{\ k}\left(dt\right)^{(3/D_F)-1}dt\end{aligned} \tag{16a,b}$$

If we divide by dt and neglect the terms which contain differential factors (for details on the method see (Casian Botez et al., 2010; Agop et al. 2008)), the equations (16a,b) are reduced to:

$$\frac{d_{\pm}T}{dt}=\frac{\partial T}{\partial t}+\boldsymbol{V}_{\pm}\cdot\nabla T+\frac{1}{2}\frac{\partial^2 T}{\partial X^i\partial X^j}\lambda_{\pm}{}^i\lambda_{\pm}{}^j(dt)^{(2/D_F)-1}+ \\ +\frac{1}{6}\frac{\partial^3 T}{\partial X^i\partial X^j\partial X^k}\lambda_{\pm}{}^i\lambda_{\pm}{}^j\lambda_{\pm}{}^k(dt)^{(3/D_F)-1} \tag{17a,b}$$

These relations also allows us to define the operator:

$$\frac{d_{\pm}}{dt}=\frac{\partial}{\partial t}+\boldsymbol{V}_{\pm}\cdot\nabla+\frac{1}{2}\frac{\partial^2}{\partial X^i\partial X^j}\lambda_{\pm}{}^i\lambda_{\pm}{}^j(dt)^{(2/D_F)-1}+ \\ +\frac{1}{6}\frac{\partial^3}{\partial X^i\partial X^j\partial X^k}\lambda_{\pm}{}^i\lambda_{\pm}{}^j\lambda_{\pm}{}^k(dt)^{(3/D_F)-1} \tag{18a,b}$$

Under these circumstances, let us calculate $\left(\hat{\partial}T/\partial t\right)$. Taking into account equations (18a,b), (5) and (6) we obtain:

$$\begin{aligned}
\frac{\hat{\partial}T}{\partial t}&=\frac{1}{2}\left[\frac{d_+T}{dt}+\frac{d_-T}{dt}-i\left(\frac{d_+T}{dt}-\frac{d_-T}{dt}\right)\right]=\frac{1}{2}\frac{\partial T}{\partial t}+\frac{1}{2}\boldsymbol{V}_+\cdot\nabla T+\\
&+\lambda_+^i\lambda_+^j\frac{1}{4}(dt)^{(2/D_F)-1}\frac{\partial^2 T}{\partial X^i\partial X^j}+\lambda_+^i\lambda_+^j\lambda_+^k\frac{1}{12}(dt)^{(3/D_F)-1}\frac{\partial^3 T}{\partial X^i\partial X^j\partial X^k}+\\
&+\frac{1}{2}\frac{\partial T}{\partial t}+\frac{1}{2}\boldsymbol{V}_-\cdot\nabla T+\lambda_-^i\lambda_-^j\frac{1}{4}(dt)^{(2/D_F)-1}\frac{\partial^2 T}{\partial X^i\partial X^j}+\\
&+\lambda_-^i\lambda_-^j\lambda_-^k\frac{1}{12}(dt)^{(3/D_F)-1}\frac{\partial^3 T}{\partial X^i\partial X^j\partial X^k}-\frac{i}{2}\frac{\partial T}{\partial t}-\frac{i}{2}\boldsymbol{V}_+\cdot\nabla T-\\
&-\lambda_+^i\lambda_+^j\frac{i}{2}(dt)^{(2/D_F)-1}\frac{\partial^2 T}{\partial X^i\partial X^j}-\lambda_+^i\lambda_+^j\lambda_+^k\frac{i}{12}(dt)^{(3/D_F)-1}\frac{\partial^3 T}{\partial X^i\partial X^j\partial X^k}+\\
&+\frac{i}{2}\frac{\partial T}{\partial t}+\frac{i}{2}\boldsymbol{V}_-\cdot\nabla T+\lambda_-^i\lambda_-^j\frac{i}{2}(dt)^{(2/D_F)-1}\frac{\partial^2 T}{\partial X^i\partial X^j}+\\
&+\lambda_-^i\lambda_-^j\lambda_-^k\frac{i}{12}(dt)^{(3/D_F)-1}\frac{\partial^3 T}{\partial X^i\partial X^j\partial X^k}=\\
&=\frac{\partial T}{\partial t}+\left(\frac{\boldsymbol{V}_++\boldsymbol{V}_-}{2}-i\frac{\boldsymbol{V}_++\boldsymbol{V}_-}{2}\right)\cdot\nabla T+\\
&+\frac{(dt)^{(2/D_F)-1}}{4}\left[\left(\lambda_+^i\lambda_+^j+\lambda_-^i\lambda_-^j\right)-i\left(\lambda_+^i\lambda_+^j-\lambda_-^i\lambda_-^j\right)\right]\frac{\partial^2 T}{\partial X^i\partial X^j}+\\
&+\frac{(dt)^{(3/D_F)-1}}{12}\left[\left(\lambda_+^i\lambda_+^j\lambda_+^k+\lambda_-^i\lambda_-^j\lambda_-^k\right)-i\left(\lambda_+^i\lambda_+^j\lambda_+^k-\lambda_-^i\lambda_-^j\lambda_-^k\right)\right]\frac{\partial^3 T}{\partial X^i\partial X^j\partial X^k}=\\
&=\frac{\partial T}{\partial t}+\hat{\boldsymbol{V}}\cdot\nabla T+\frac{(dt)^{(2/D_F)-1}}{4}\left[\left(\lambda_+^i\lambda_+^j+\lambda_-^i\lambda_-^j\right)-i\left(\lambda_+^i\lambda_+^j-\lambda_-^i\lambda_-^j\right)\right]\frac{\partial^2 T}{\partial X^i\partial X^j}+\\
&+\frac{(dt)^{(3/D_F)-1}}{12}\left[\left(\lambda_+^i\lambda_+^j\lambda_+^k+\lambda_-^i\lambda_-^j\lambda_-^k\right)-i\left(\lambda_+^i\lambda_+^j\lambda_+^k-\lambda_-^i\lambda_-^j\lambda_-^k\right)\right]\frac{\partial^3 T}{\partial X^i\partial X^j\partial X^k}
\end{aligned} \tag{19a,b}$$

This relation also allows us to define the fractal operator:

$$\frac{\hat{\partial}}{\partial t}=\frac{\partial}{\partial t}+\hat{\boldsymbol{V}}\cdot\nabla+\frac{(dt)^{(2/D_F)-1}}{4}\left[\left(\lambda_+^i\lambda_+^j+\lambda_-^i\lambda_-^j\right)-i\left(\lambda_+^i\lambda_+^j-\lambda_-^i\lambda_-^j\right)\right]\frac{\partial^2}{\partial X^i\partial X^j}+$$
$$+\frac{(dt)^{(3/D_F)-1}}{12}\left[\left(\lambda_+^i\lambda_+^j\lambda_+^k+\lambda_-^i\lambda_-^j\lambda_-^k\right)-i\left(\lambda_+^i\lambda_+^j\lambda_+^k-\lambda_-^i\lambda_-^j\lambda_-^k\right)\right]\frac{\partial^3}{\partial X^i\partial X^j\partial X^k} \tag{20}$$

Particularly, by choosing:

$$\lambda_+^i\lambda_+^j=-\lambda_-^i\lambda_-^j=2\mathsf{D}\delta^{ij}$$
$$\lambda_+^i\lambda_+^j\lambda_+^k=\lambda_-^i\lambda_-^j\lambda_-^k=2\sqrt{2}\mathsf{D}^{3/2}\delta^{ijk} \tag{21a,b}$$

the fractal operator (20) takes the usual form:

$$\frac{\hat{\partial}}{\partial t}=\frac{\partial}{\partial t}+\hat{\boldsymbol{V}}\cdot\nabla-i\mathsf{D}(dt)^{(2/D_F)-1}\Delta+\frac{\sqrt{2}}{3}\mathsf{D}^{3/2}(dt)^{(3/D_F)-1}\nabla^3 \tag{22}$$

We now apply the principle of scale covariance, and postulate that the passage from classical (differentiable) mechanics to the "fractal" mechanics can be implemented by replacing the standard time derivative operator, d/dt, by the complex operator $\hat{\partial}/\partial t$ (this results in a generalization of the principle of scale covariance given by Nottale in (Nottale, 1992)). As a consequence, we are now able to write the equation of the heat flow in its covariant form:

$$\frac{\hat{\partial}T}{\partial t}=\frac{\partial T}{\partial t}+\left(\hat{\boldsymbol{V}}\cdot\nabla\right)T-i\mathsf{D}(dt)^{(2/D_F)-1}\Delta T+\frac{\sqrt{2}}{3}\mathsf{D}^{3/2}(dt)^{(3/D_F)-1}\nabla^3T=0 \tag{23}$$

This means that at any point of a fractal heat flow path, the local temporal term, $\partial_t T$, the non-linearly (convective) term, $\left(\hat{\boldsymbol{V}}\cdot\nabla\right)T$, the dissipative term, ΔT and the dispersive one, ∇^3T, make their balance. Moreover, the behavior of a fractal fluid is of viscoelastic or of hysteretic type, *i.e.* the fractal fluid has memory. Such a result is in agreement with the opinion given in (Ferry& Goodnick, 1997; Chiroiu et al., 2005): the fractal fluid can be described by Kelvin-Voight or Maxwell rheological model with the aid of complex quantities e.g. the complex speed field, the complex structure coefficients.

4. The dissipative approximation in the heat transfer processes

4.1 Standard thermal transport

In the dissipative approximation of the fractal heat transfer, the relation (23) becomes a Navier-Stokes type equation for the temperature field:

$$\frac{\hat{\partial}T}{\partial t}=\frac{\partial T}{\partial t}+\left(\hat{\boldsymbol{V}}\cdot\nabla\right)T-i\mathsf{D}(dt)^{(2/D_F)-1}\Delta T=0 \tag{24}$$

with an imaginary viscosity coefficient:

$$\eta=i\mathsf{D}(dt)^{2/D_F-1} \tag{25}$$

Separating the real and imaginary parts in (24), *i.e.*

$$\begin{aligned} &\frac{\partial T}{\partial t}+\boldsymbol{V}\cdot\nabla T=0 \\ &-\boldsymbol{U}\cdot\nabla T=\mathsf{D}\left(dt\right)^{(2/D_F)-1}\Delta T \end{aligned} \tag{26a,b}$$

We can add these two equations and obtain the thermal transfer equation in the form:

$$\frac{\partial T}{\partial t}+(\boldsymbol{V}-\boldsymbol{U})\cdot\nabla T=\mathsf{D}\left(dt\right)^{(2/D_F)-1}\Delta T \tag{27}$$

The standard equation for the thermal transport, *i.e.*:

$$\frac{\partial T}{\partial t}=\alpha\Delta T,\quad \alpha=\mathsf{D}\left(dt\right)^{(2/D_F)-1} \tag{28a,b}$$

results from (27) on the following assertions

i. the fractal heat flow are of Peano's type (Nottale, 1992), i.e. for $D_F=2$;
ii. the movements at differentiable and non-differentiable scales are synchronous, i.e. $\boldsymbol{V}=\boldsymbol{U}$;
iii. the structure coefficient D, proper to the fractal-nonfractal transition, is identified with the diffusivity coefficient α, i.e. $\alpha\equiv\mathsf{D}$.

In the form

$$\frac{\partial\overline{T}}{\partial t}=\left(\frac{\partial^2}{\partial\overline{x}^2}+\frac{\partial^2}{\partial\overline{y}^2}\right)\overline{T} \tag{29}$$

where we used the normalized quantities

$$\overline{t}=\omega t,\quad \overline{x}=kx,\quad \overline{y}=ky,\quad \overline{T}=\frac{T}{T_0} \tag{30a-d}$$

and the restriction

$$\frac{\mathsf{D}k^2}{\omega}=1 \tag{31}$$

the equation (29) can by solved with the following initial and boundaries conditions:

$$\overline{T}\left(0,\overline{x},\overline{y}\right)=\frac{1}{4},\text{for } 0\le\overline{x}\le 1 \text{ and } 0\le\overline{y}\le 1 \tag{32a,b}$$

$$\begin{aligned} &\overline{T}\left(\overline{t},0,\overline{y}\right)=1/4\,,\overline{T}\left(\overline{t},1,\overline{y}\right)=1/4 \\ &\overline{T}\left(\overline{t},\overline{x},0\right)=\exp\left[-\left(\frac{\overline{t}-1/2}{1/2}\right)^2\right]\exp\left[-\left(\frac{\overline{x}-1/2}{1/2}\right)^2\right],\overline{T}\left(\overline{t},\overline{x},1\right)=1/4 \end{aligned} \tag{33a-d}$$

In the Figures (1a-j) we present the solutions obtained with the finite differences method (Zienkievicz &Taylor, 1991). Furthermore, using tha same method from (Zienkievicz

&Taylor, 1991), if the thermal transport occurs in the presence of a "wall", condition which involves substituting (33d) with

$$\frac{\partial \overline{T}}{\partial \overline{y}}\left(\overline{t},\overline{x},1\right)=0 \tag{34}$$

then obtain the numerical solutions from the figures (2a-j). It results that the perturbation of the thermal field, either disappear because of the rheological properties of the fractal environment (Figures 1a-j), or it regenerates (Figures 2a-j).

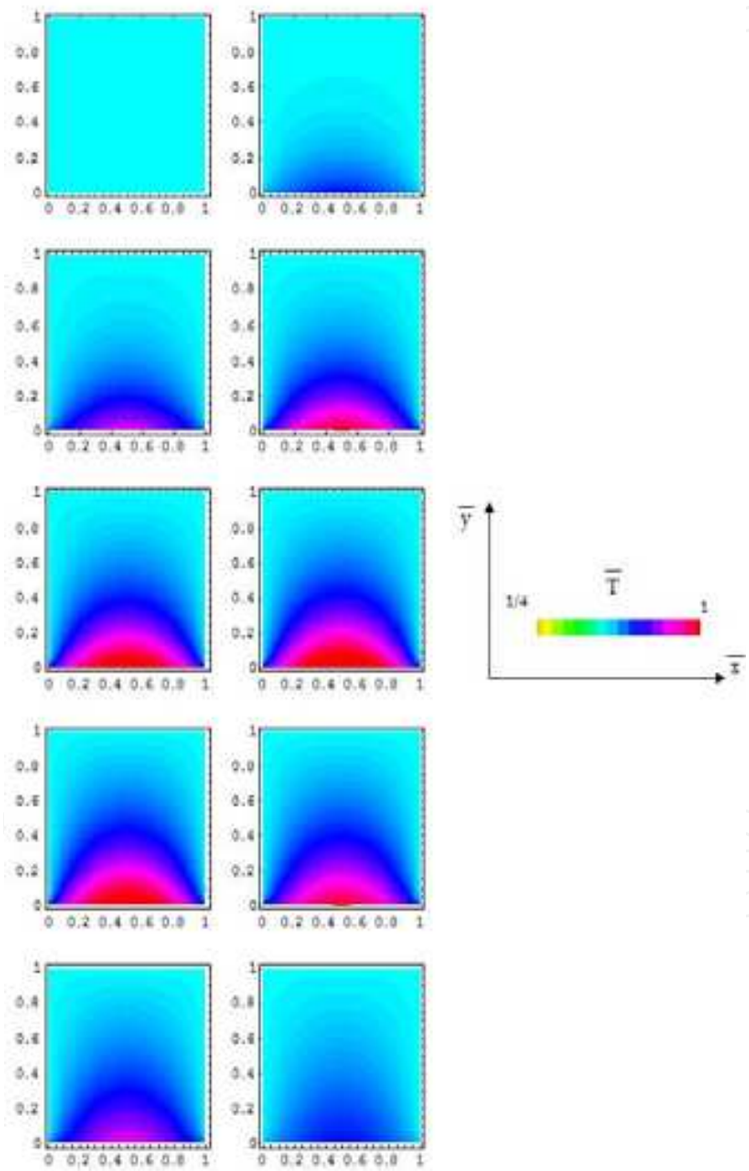

Fig. 1. a-j. Numerical 2D contour curves of the normalized temperature field in the absence of a "wall". Thermal field perturbation disappears due to the rheological properties of the fractal environment

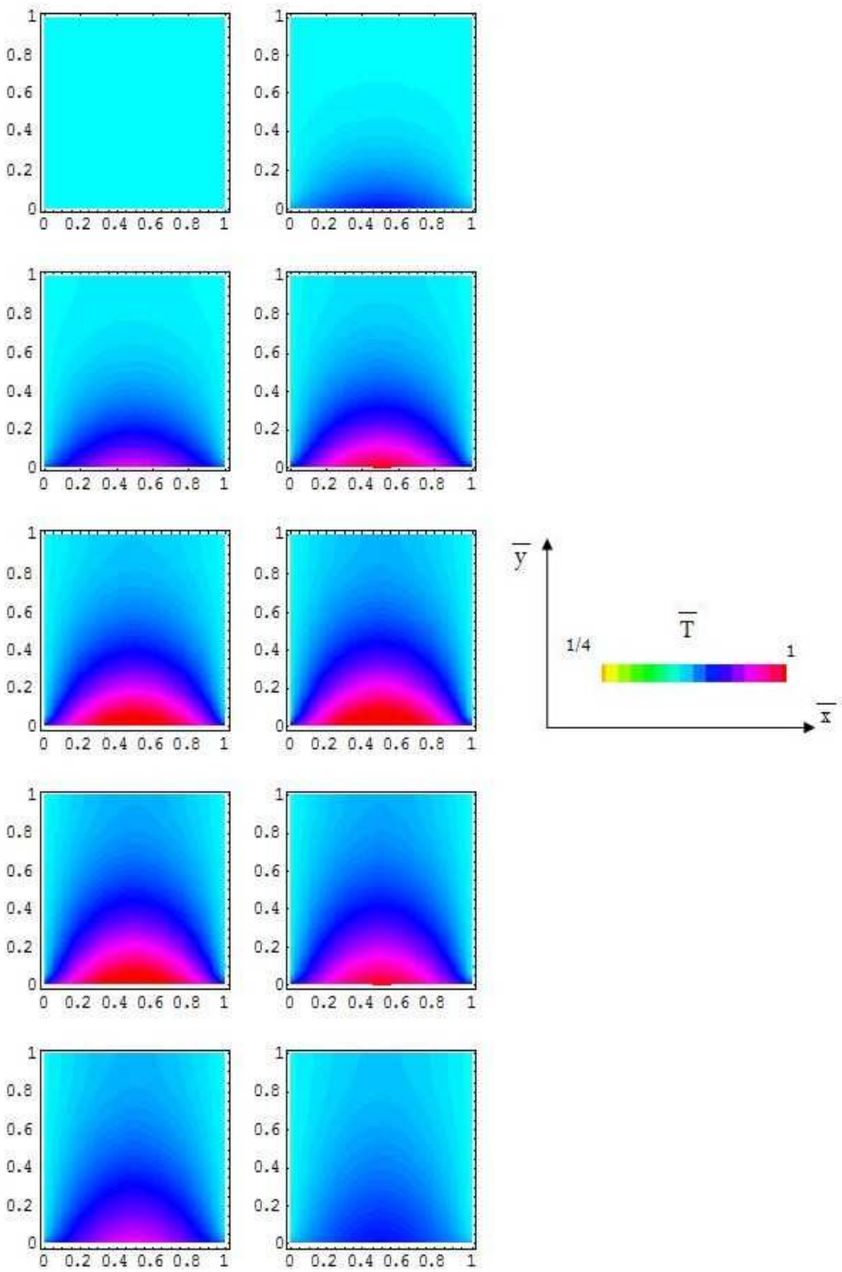

Fig. 2. a-j. Numerical 2D contour curves of the normalized temperature field in the presence of a "wall". Thermal field perturbation regenerates in the presence of a "wall"

4.2 Thermal anomaly of the nanofluids

The equation (28a) is implied by the Fourier type law

$$\boldsymbol{j}(T) = -k\nabla T \tag{35}$$

with $\boldsymbol{j}(T)$ the thermal current density and k the thermal conductivity.

Let us apply the previous formalism for the heat transfer in nanofluids, assuming the following: (i) there are two different paths (fractal curves of fractal dimension D_F) of heat flow through the "suspension", one through the fluid particles and other through the nanoparticles; (ii) the fractal curves are of Peano type (Nottale, 1992), which implies D_F=2. The overall heat transfer rate of the system, q, for the one-dimensional heat flow, may be expressed as:

$$q = q_f + q_p = -k_f A_f \left(\frac{dT}{dX}\right)_f - k_p A_p \left(\frac{dT}{dX}\right)_p \tag{36}$$

where A, k, (dT/dX) denote the heat transfer area, the thermal conductivity and the temperature gradient, while the subscripts f, p denote quantities corresponding to the fluid and the particle phase, respectively. Assuming that the fluid and the nanoparticles are in local thermal equilibrium at each location, we can set:

$$\left(\frac{dT}{dX}\right)_f = \left(\frac{dT}{dX}\right)_p = \left(\frac{dT}{dX}\right) \tag{37}$$

Now the overall heat transfer rate can be expressed as

$$q_t = -k_f A_f \left(\frac{dT}{dX}\right)\left[1 + \frac{k_p A_p}{k_f A_f}\right] \tag{38}$$

We propose, using the method from (Hemanth Kumar et al., 2004), that the ratio of heat transfer areas, $\left(A_p/A_f\right)$, could be taken in proportion to the total surface areas of the nanoparticles $\left(S_p\right)$ and the fluid species $\left(S_f\right)$ per unit volume of the "suspension". Taking both the fluid and the suspended nanoparticles to be spheres of radii r_f and r_p respectively, the total surface area can be calculated as the product of the number of particles n and the surface area of the particle for each constituent. Denoting by ε the volume fraction of the nanoparticle and by $(1-\varepsilon)$ the volume fraction of the fluid, the number of particles for the two constituents can be calculated as :

$$n_f = \frac{1}{\frac{4}{3}\pi r_f^3}(1-\varepsilon)$$
$$n_p = \frac{1}{\frac{4}{3}\pi r_p^3}\varepsilon \tag{39a,b}$$

The corresponding surface areas of the fluid and the nanoparticle phase are given by:

$$S_f = n_f 4\pi\left(r_f\right)^2 = \frac{3}{r_f}(1-\varepsilon)$$
$$S_p = n_p 4\pi\left(r_p\right)^2 = \frac{3}{r_p}\varepsilon \tag{40a,b}$$

Taking

$$\frac{S_f}{S_p}=\frac{A_f}{A_p} \tag{41}$$

and using the previous relations, the expression for the heat transfer rate becomes:

$$q=-k_f A_f\left(\frac{dT}{dX}\right)\left[1+\frac{k_p\varepsilon r_f}{k_f(1-\varepsilon)r_p}\right]=-k_{ef}A_f\left(\frac{dT}{dX}\right) \tag{42}$$

where the effective thermal conductivity, k_{eff} is expressed as:

$$\frac{k_{eff}}{k_f}=1+\frac{k_p\varepsilon r_f}{k_f(1-\varepsilon)r_p} \tag{43}$$

We present in Figures 3a-c the dependencies: $k_{\text{...}}/k_{\text{.}}\left(k_{\text{..}}/k_f=\text{const.},\varepsilon,r_p/r_f\right)$ (a), $k_{eff}/k_f\left(k_p/k_f,\varepsilon,r_p/r_f=\text{const.}\right)$ (b) and $k_{eff}/k_f\left(k_p/k_f,\varepsilon=\text{const.},r_p/r_f\right)$ (c).
In the above expression, it is seen that the enhancement is directly proportional to the ratio of the conductivities, volume fraction of the nanoparticle (for $\varepsilon\ll 1$) and is inversely proportional to the nanoparticle radius.
Next we determine the temperature dependence of k_{eff}. The thermal conduction of nanoparticle based on Debye's model is:

$$k_p=\frac{n\hat{c}_v l}{3}\left\langle u_p\right\rangle \tag{44}$$

where l is the mean free path, $\hat{c}_v$ is the specific heat per particle, n is the particle concentration and $\left\langle u_p\right\rangle$ the average particle speed. Because the particle's movement in fluid is a Brownian one, so it can be approximate by a fractal with fractal dimension $D_F=2$, we can use a Stokes-Einstein's type formula for the definition of D from Eqs. (21a, b)

$$\mathsf{D}\sim\frac{k_B T}{\pi\eta r_p} \tag{45}$$

with k_B the Boltzmann's constant, T the temperature and η the dynamic viscosity of the fluid. For a choice of the form:

$$\mathsf{D}\sim\left\langle u_p(T)\right\rangle r_p \tag{46}$$

which implies

$$\left\langle u_p(T)\right\rangle\sim\frac{k_B T}{\pi\eta r_p^2} \tag{47}$$

the equation (44) becomes:

$$k_p\sim k_p(T_0)t_r,\ t_r=\frac{T}{T_0},\ k_p(T_0)=\frac{n\hat{C}_v l}{3}\left\langle u_p(T_0)\right\rangle,\ \left\langle u_p(T_0)\right\rangle\sim\frac{k_B T_0}{\pi\eta r_p^2} \tag{48a-d}$$

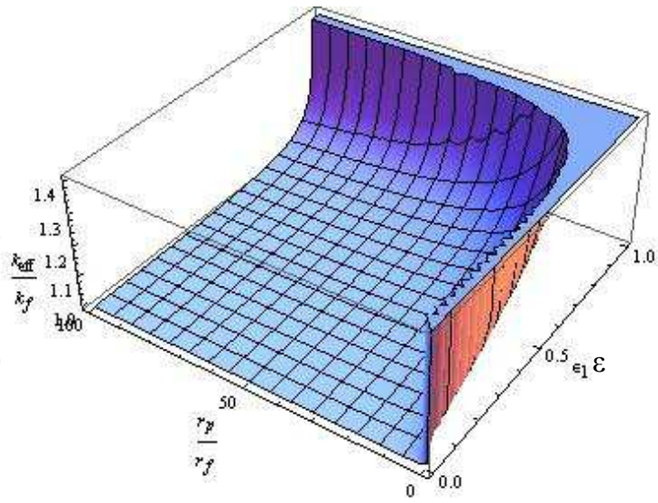

a)

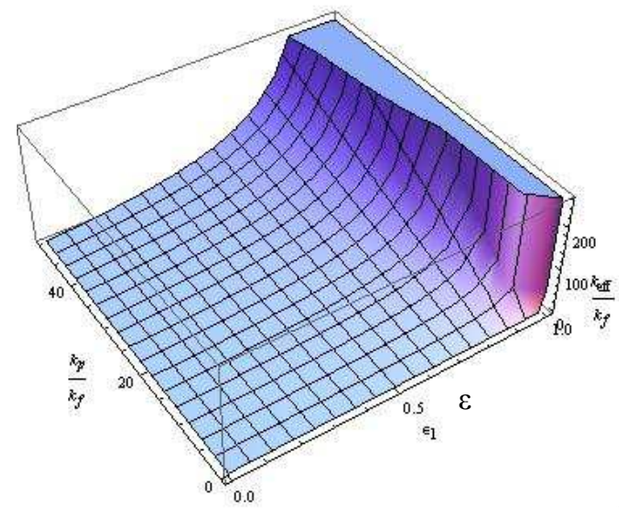

b)

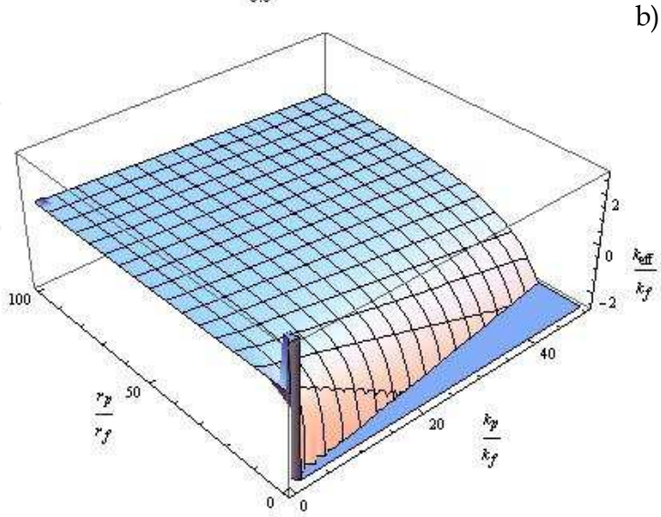

c)

Fig. 3. Dependence of the effective thermal conductivity k_{eff} on: (a) $r_p/r_f, \varepsilon$; (b) $k_p/k_f, \varepsilon$; (c) $r_p/r_f, k_p/k_f$

So, the dependence of k_{eff} on the reduced temperature t_r takes the form (see also Fig.4):

$$\frac{k_{eff}}{k_f} = 1 + \nu t_r, \nu = \frac{k_p(T_0)\varepsilon r_f}{k_f(1-\varepsilon)r_p} \tag{49a,b}$$

Obviously, Eq.(49a) it more complicated if we accept the dependence $\eta = \eta(t_r)$.

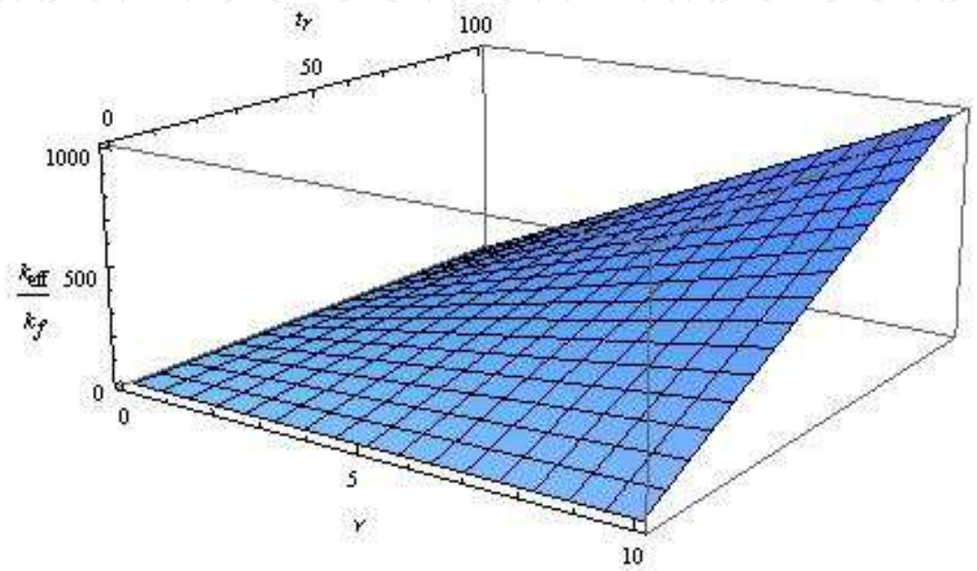

Fig. 4. Dependence of the effective thermal conductivity k_{eff} on the reduced temperature t_r and ν

We remark that the theoretical model describes not only qualitative but also quantitative the thermal behavior of the nanofluids experimentally observed (the increasing of the heat transfer in nanofluids-thermal anomaly of the nanofluids) (Wang&Xu, 1999; Keblinski, 2002; Hemanth Kumar et al., 2004).

4.3 Negative differential thermal conductance effect

Applying the fractal operator (22) in the dispersive approximation of motions to the complex speed field (fractal function), $\hat{\boldsymbol{V}}$ we obtain the inertial principle in the form of a Navier-Stokes type equation:

$$\frac{\hat{\partial} T}{\partial t} = \frac{\partial T}{\partial t} + \hat{\boldsymbol{V}} \cdot \nabla T + \frac{\sqrt{2}}{3} \mathsf{D}^{3/2} (dt)^{(3/D_F)-1} \nabla^3 T = 0 \tag{50}$$

with a imaginary viscosity coefficient (25).

This means that the local complex acceleration field, $\partial \hat{\boldsymbol{V}} / \partial t$, the convective term, $\hat{\boldsymbol{V}} \cdot \nabla \hat{\boldsymbol{V}}$, and the dissipative one, $\nabla \hat{\boldsymbol{V}}$, reciprocally compensate in any point of the fractal curve.

In the case of the irrotational motions:

$$\nabla \times \hat{\boldsymbol{V}} = 0 \tag{51}$$

so that the complex speed field (6) can be expressed through the gradient of a complex scalar function Φ,

$$\hat{\boldsymbol{V}} = \nabla \boldsymbol{\Phi} \tag{52}$$

named the scalar potential of the complex speed field.
Substituting equation (52) in equation (50) it results

$$\nabla\left[\frac{\partial \boldsymbol{\Phi}}{\partial t} + \frac{1}{2}\left(\nabla \boldsymbol{\Phi}\right)^2 - i\mathrm{D}\left(dt\right)^{(2/D_F)-1}\Delta \boldsymbol{\Phi}\right] = 0 \tag{53}$$

and by an integration, a Bernoulli type equation

$$\frac{\partial \boldsymbol{\Phi}}{\partial t} + \frac{1}{2}\left(\nabla \boldsymbol{\Phi}\right)^2 - i\mathrm{D}\left(dt\right)^{(2/D_F)-1}\Delta \boldsymbol{\Phi} = F\left(t\right) \tag{54}$$

with *F(t)* function which depends only on time. Particularly, for $\boldsymbol{\Phi}$ of the form:

$$\boldsymbol{\Phi} = -2i\mathrm{D}\left(dt\right)^{(2/D_F)-1}\ln\psi \tag{55}$$

where ψ is a new complex scalar function, the equation (54) takes the form:

$$\mathrm{D}^2\left(dt\right)^{(4/D_F)-1}\Delta\psi + i\mathrm{D}\left(dt\right)^{(2/D_F)-1}\frac{\partial \psi}{\partial t} + \frac{F\left(t\right)}{2}\psi = 0 \tag{56}$$

From here, a Schrödinger type equation result for $F(t)\equiv 0$ *i.e.*

$$\mathrm{D}^2\left(dt\right)^{(4/D_F)-1}\Delta\psi + i\mathrm{D}\left(dt\right)^{(2/D_F)-1}\frac{\partial \psi}{\partial t} = 0 \tag{57}$$

Moreover, for the movement on fractal curves of Peano's type, *i.e.* in the fractal dimension $D_F = 2$, and Compton's length, λ, and temporal, τ, scales,

$$\lambda = \frac{\hbar}{m_0 c}$$

$$\tau = \frac{\hbar}{m_0 c^2} \tag{58a,b}$$

equation (57) takes the Schrödinger standard form:

$$\frac{\hbar^2}{2m_0}\Delta\psi + i\hbar\frac{\partial \psi}{\partial t} = 0 \tag{59}$$

In the relations (58 a,b) and (59) $\hbar$ is the reduced Plank's constant, c the speed of light on the vacuum and m_0 the rest mass of the particle test.
Let us apply the previous mathematical model in the description of two fractal fluids interface dynamics in the fractal dimension D_F. Consider two fractal fluids, 1 and 2, separated by an interface as shown in Figure 5. If the interface is thick enough so that the

fractal fluids are "isolated" from each other, the time-dependent Schrödinger type equation for each side is:

$$im_0 2D\frac{d\psi_1}{dt} = H_1\psi_1 \tag{60}$$

$$im_0 2D\frac{d\psi_2}{dt} = H_2\psi_2 \tag{61}$$

with

$$D = \mathsf{D}(dt)^{(2/D_F)-1} \tag{62}$$

where ψ_i and H_i, i = 1, 2 are the scalar potentials of the complex speed fields and respectively the "Hamiltonians" on either side of the interface. We assume that a temperature field, 2T, is applied between the two fractal fluids. If the zero point of the temperature field is assumed to occur in the middle of the interface, the fractal fluid 1 will be at the temperature field -T, while the fractal fluid 2 will be at the temperature field +T.

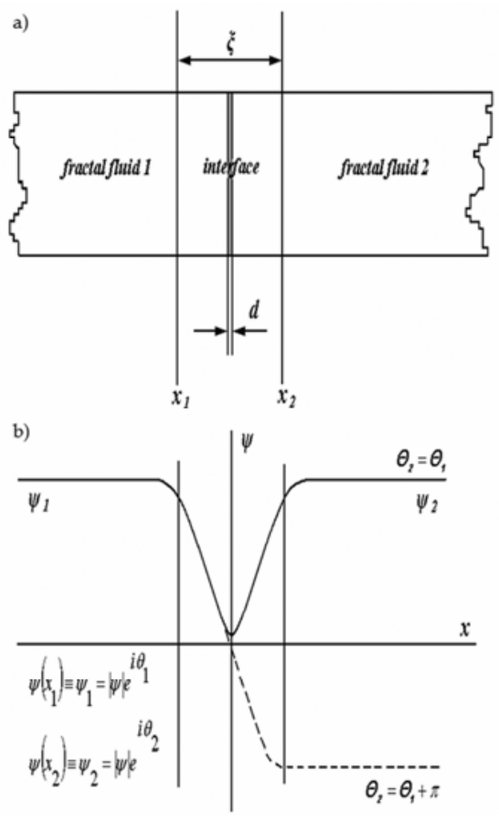

Fig. 5. Interface generated through the interaction of two fractal fluids (d is the geometrical thickness, before the self-structuring of the interface and ξ is the physical thickness, after the self-structuring of the interface) (a) and the variation of the speed field with the fractal coordinates (b)

The presence of the interface couples together the two previous Equations (60) and (61) in the form:

$$im_0 2D\frac{d\psi_1}{dt} = \alpha T\psi_1 + \Gamma\psi_2 \tag{63}$$

$$im_0 2D\frac{d\psi_2}{dt} = -\alpha T\psi_2 + \Gamma\psi_1 \tag{64}$$

where a is a constant which specifies the thermal transfer type in the fractal fluid (Vizureanu&Agop, 2007) and Γ is the coupling constant for the scalar potentials of the complex speed fields across the interface. Since the square of each scalar potential of the complex speed fields is also a probability density (Notalle, 1992, 2008a, 2008b, 2007), the two scalar potentials of the complex speed fields can be written in the form:

$$\psi_1 = \sqrt{\rho_1}e^{i\theta_1} \tag{65}$$

$$\psi_2 = \sqrt{\rho_2}e^{i\theta_2} \tag{66}$$

$$\Theta = \theta_2 - \theta_1 \tag{67}$$

where ρ_1 and ρ_2 are the densities of particles in the two fractal fluids and Θ is the phase difference across the interface. If the two scalar potentials of the complex speed fields (65) and (66) are substituted in the coupled Equations (63) and (64) and the results separated into real and imaginary parts, we obtain equations for the time dependence of the particle densities and the phase difference:

$$\frac{d\rho_1}{dt} = -\frac{\Gamma}{m_0 D}\sqrt{\rho_1\rho_2}\sin\Theta \tag{68}$$

$$\frac{d\rho_2}{dt} = -\frac{\Gamma}{m_0 D}\sqrt{\rho_1\rho_2}\sin\Theta \tag{69}$$

$$\frac{d\Theta}{dt} = \frac{\alpha T}{m_0 D} = \overline{\Omega} \tag{70}$$

We can specify the heat flux in terms of the difference between Equations (69) and (70) which multiplies with ε:

$$j = \varepsilon\frac{d}{dt}(\rho_1 - \rho_2) \tag{71}$$

It results

$$j = j_c\sin\Theta \tag{72}$$

where

$$j_c = \frac{2\varepsilon\Gamma\sqrt{\rho_1\rho_2}}{m_0 D} \tag{73}$$

and ε is the elementary amount of energy transferred trough the interface (Vizureanu&Agop, 2007).
Equations (70) and (72) define the thermal transport inside the interface. If the temperature field from Equation (70) is zero, a constant heat flux of any value between $-j_c$ and j_c may flow through the junction according to the Equation (72).
We return to Equations (69), (70) and (72) and apply a constant temperature field T_0 to the junction that is:

$$\Theta(t) = \frac{\alpha}{m_0 D} T_0 t + \Theta_0 , \ \Theta_0 = \text{const.} \tag{74a,b}$$

A variable heat flux:

$$j(t) = j_c \sin\left(\Omega_0 t + \Theta_0\right)$$

$$\Omega_0 = \frac{\alpha}{m_0 D} T_0 \tag{75 a,b}$$

results, although a constant temperature field is applied.
If one overlay an "alternative" temperature field over the constant temperature field:

$$T(t) = T_0 + \overline{T}_0 \cos\left(\Omega t\right) \tag{76}$$

one obtains a "frequency" modulation of the "heat flux":

$$j = j_c \sin\left(\Omega_0 t + \frac{\alpha \overline{T}_0}{m_0 \Omega D} s\text{in}\left(\Omega t\right) + \overline{\Theta}_0 \right) =$$
$$= j_C \sum_{n=-\infty}^{+\infty} (-1)^n J_n \left(\frac{\alpha \overline{T}_0}{m_0 \Omega D} \right) \sin\left[\left(\Omega_0 - n\Omega\right) t + \overline{\Theta}_0 \right]$$

$$\overline{\Theta}_0 = \text{const.} \tag{77a,b}$$

J_n is the Bessel function of integer index (Nikitov&Ouvanov, 1974). We note that, in the first approximation, for any "arbitrary" thermal signal we can always perform a Fourier's decomposition (Jackson, 1991).
Since j versus T characteristic is drawn for the average thermal flux $j \approx \langle j(t) \rangle$, and since the sine term averages to zero unless $\Omega_0 = n\Omega$, there are spikes appearing on this characteristic for temperature field equal to:

$$T_n = n \frac{m_0 D}{\alpha} \Omega \tag{78}$$

with the maximum amplitude

$$j_{\max} = j_c J_n \left(\frac{\alpha \overline{T}_0}{m_0 \Omega D} \right) \tag{79}$$

occurring for the phase $\bar{\Theta} = \pi/2$. Figure 6 shows these spikes at intervals proportional to the thermal source "frequency" and indicates their maximum amplitude range. The value of the heat flux can be anywhere along a particular heat flux spike, depending on the initial phase.

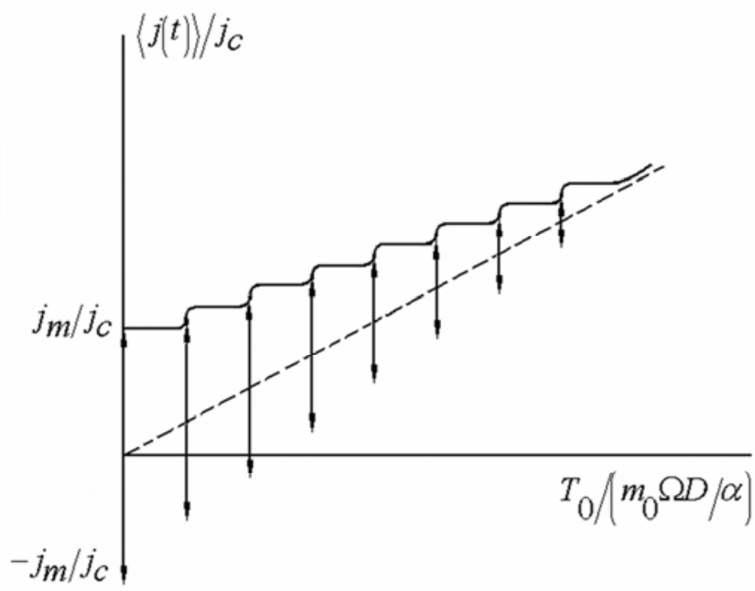

Fig. 6. Theoretical heat flux-temperature characteristic

It results the following:

i. The presence of the spikes in the average heat flux specifies a negative differential thermal "conductance" which corresponds to the interface self-structuring. This is a Josephson thermal type effect;
ii. Condition (78) corresponds to the "modulation" of the interface "oscillations" under the influence of an external thermal signal.

4.4 Numerical simulations of the heat transfer in nanofluids

Replacing the complex speed field (6) in equation (50) and separating the real and imaginary parts, we obtain:

$$m_0 \frac{\partial \boldsymbol{V}}{\partial t} + m_0 \boldsymbol{V} \cdot \nabla \boldsymbol{V} = -\nabla (Q)$$
$$\frac{\partial \boldsymbol{U}}{\partial t} + \nabla (\boldsymbol{V} \cdot \boldsymbol{U}) + D(dt)^{(2/D_F)-1} \Delta \boldsymbol{V} = 0 \qquad (80a,b)$$

where Q is the fractal potential,

$$Q = -\frac{m_0 \boldsymbol{U}^2}{2} - m_0 D(dt)^{(2/D_F)-1} \nabla \cdot \boldsymbol{U} \qquad (81)$$

The explicit form of the complex speed field is given by means the expression:

$$\psi = \sqrt{\rho}\, e^{iS} \qquad (82)$$

with ρ the amplitude and S the phase. Then equation (55) with

$$\Phi = -2iD(dt)^{(2/D_F)-1} \ln\left(\sqrt{\rho}\, e^{iS}\right) \tag{83}$$

involves the real and imaginary speed field components

$$\begin{aligned} \boldsymbol{V} &= 2D(dt)^{(2/D_F)-1} \nabla S \\ \boldsymbol{U} &= D(dt)^{(2/D_F)-1} \nabla \ln \rho \end{aligned} \tag{84a,b}$$

while the fractal potential (81) is given by the simple expression

$$Q = -m_0 D^2 (dt)^{(4/D_F)-2} \frac{\Delta\sqrt{\rho}}{\sqrt{\rho}} \tag{85}$$

With equations (84 a, b), the relation (80 b) takes the form:

$$\nabla\left(\frac{\partial \ln \rho}{\partial t} + \boldsymbol{V}\cdot\nabla \ln \rho + \nabla\cdot\boldsymbol{V}\right) = 0 \tag{86}$$

or, by integration with $\rho \neq 0$:

$$\frac{\partial \rho}{\partial t} + \nabla\cdot(\rho \boldsymbol{V}) = T(t) \tag{87}$$

with $T(t)$ a function which depends only on time.
Equation (80 a) corresponds to the momentum conservation law, while equation (87), with $T(t)\equiv 0$ to the probability density conservation law. So, equations:

$$\begin{aligned} m_0\left(\frac{\partial \boldsymbol{V}}{\partial t} + \boldsymbol{V}\cdot\nabla\boldsymbol{V}\right) &= -\nabla(Q) \\ \frac{\partial \rho}{\partial t} + \nabla\cdot(\rho\boldsymbol{V}) &= 0 \end{aligned} \tag{88a,b}$$

with Q given by (81) or (85), from the fractal hydrodynamic equations in the fractal dimension D_F. The fractal potential (81) is induced by the non-differentiability of the space coordinates.
Now, by multiplying equation (88 b) with ε, *i.e.*

$$\frac{\partial(\rho\varepsilon)}{\partial t} + \nabla\cdot(\rho\varepsilon\boldsymbol{V}) = \rho\left(\frac{\partial \varepsilon}{\partial t} + \boldsymbol{V}\cdot\nabla\varepsilon\right) \tag{89}$$

and considering the null value of the right term of Eq. (89), the conservation law for ε is found in the form:

$$\frac{\partial(\rho\varepsilon)}{\partial t} + \nabla\cdot(\rho\varepsilon\boldsymbol{V}) = 0 \tag{90}$$

Particularly, if ε is the energy density of a fluid (Landau&Lifshitz, 1987), $\varepsilon=e+(p/\rho)+v^2/2$, the "classical" form of the energy conservation law results (the physical significances of e and p are given in (Landau&Lifshitz, 1987)).

Several numerical investigations of the nanofluid heat transfer have been accomplished in (Maiga et al., 2005, 2004; Patankar, 1980). Akbarnia and Behzadmehr (Akbarnia & Behzadmehr, 2007) reported a Computational Fluid Dynamics (CFD) model based on single phase model for investigation of laminar convection of water-Al_2O_3 nanofluid in a horizontal curved tube. In their study, effects of buoyancy force, centrifugal force and nanoparticle concentration have been discussed.

In that follows we shall perform numerical studies on the nanofluid heat transfer (water-based nanofluids, Al_2O_3 with 10 nm particle-sizes) in a coaxial heat exchanger.

The detailed turbulent flow field for the single-phase flow in a circular tube with constant wall temperature can be determined by solving the volume-averaged fluid equations, as follows:

i. continuity equations (88 b)

$$\frac{\partial \rho}{\partial t}+\nabla(\rho \boldsymbol{V})=0 \tag{91}$$

ii. momentum equation (88 a) in the form:

$$\frac{\partial}{\partial t}(\rho \boldsymbol{V})+\nabla(\rho \boldsymbol{V}\boldsymbol{V})=-\nabla P+\nabla \tau+B \tag{92}$$

where we supposed that (Harvey, 1966; Albeverio&Hoegh-Krohn, 1974):

$$-\nabla Q=-\nabla P+\nabla \tau+B \tag{93}$$

P, τ and B having the significances from (Fard et al., 2009);

iii. energy equation (90) in the form:

$$\frac{\partial \rho}{\partial t}(\rho H)+\nabla\left(\rho \boldsymbol{V} C_p T\right)=\nabla\left(k\nabla T-C_p \rho \boldsymbol{V} T\right) \tag{94}$$

where H is the enthalpy, C_p is the specific heat capacity and T is the temperature field.

In order to solve above-mentioned equations the thermo physical parameters of nanofluids such as density, heat capacity, viscosity, and thermal conductivity must be evaluated. These parameters are defined as follows:

i. density and heat capacity. The relations determinate by Pak si Cho (Pak&Cho, 1998), have the form:

$$\rho_{nf}=(1-\varepsilon)\rho_f+\varepsilon\rho_p \tag{95}$$

$$C_{nf}=(1-\varepsilon)C_f+\varepsilon C_p \tag{96}$$

ii. thermal conductivity. The effective thermal conductivity of a mixture can be calculated by using relation (43):

$$\frac{k_{eff}}{k_f}=1+0.043\frac{k_p \varepsilon}{k_f(1-\varepsilon)} \tag{97}$$

where we consider that $r_f/r_p \approx 0{,}043$ as in (Kumar et al., 2004; Jang&Choi, 2004; Prasher, 2005) and $k_{eff} = k_{nf}$;

iii. viscosity. We choose the polynomial approximation based on experimental data Nguyen (Nguyen et al., 2005), for water – Al_2O_3 nanofluid:

$$\mu_{nf} = \left(306\varepsilon^2 - 0.19\varepsilon + 1\right)\mu_f \tag{98}$$

These equations were used to perform the calculation of temperature distribution and transmission fields in the geometry studied.

Figure 7 shows the geometric configuration of the studied model which consists of a coaxial heat exchanger with length *L=64 cm*; inner tube diameter *d=10 mm* and outer tube diameter *D=20 mm*. By inner tube will circulate a nanofluid as primary agent, and by the outer tube will circulate pure water as secondary agent. The nanofluid used is composed of aluminum oxide Al_2O_3 particles dispersed in pure water in different concentrations (1%, 3% and 5%).

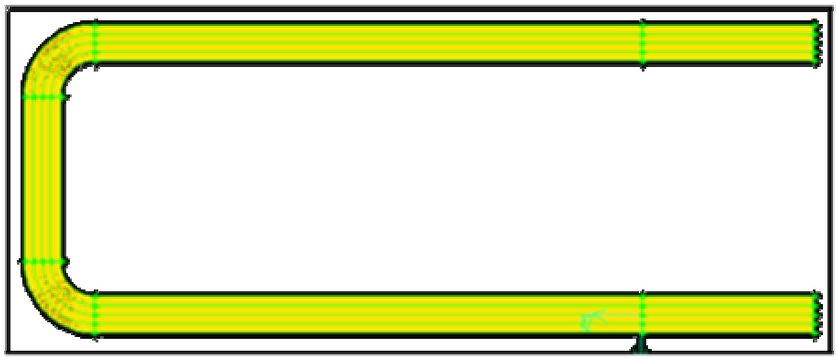

Fig. 7. Geometry of coaxial heat exchanger

The continuity, momentum, and energy equations are non-linear partial differential equations, subjected to the following boundary conditions: at the tubes inlet, "velocity inlet" boundary condition was used. The magnitude of the inlet velocity varies for the inner tube between 0,12 m/s and 0,64 m/s, remaining constant at the value of 0,21 m/s for the outer tube. Temperatures used are 60, 70, 90 degrees C for the primary agent and for the secondary agent is 30 degrees C. Heat loss to the outside were considered null, imposing the heat flux = 0 at the outer wall of heat exchanger. The interior wall temperature is considered equal to the average temperature value of interior fluid. Using this values for velocity, the flow is turbulent and we choose a corresponding model *(k-ε)* for solve the equations (Mayga&Nguyen, 2006; Bianco et al., 2009).

For mixing between the base fluid and the three types of nanofluids were performed numerical simulations to determinate correlations between flows regime, characterized by Reynold's number, and convective coefficient values.

The convective coefficient value *h* is calculated using Nusselt number for nanofluids (Al_2O_3+H_2O), relation established following experimental determinations by Vasu and all (Vasu et al., in press):

$$Nu_{nf} = 0.0023 \cdot \mathrm{Re}_{nf}^{0.8} \cdot \mathrm{Pr}_{nf}^{0.4} \tag{99}$$

where the Reynolds number is defined by:

$$\mathrm{Re}_{nf} = \frac{\rho_{nf} v_m d}{\mu_{nf}} \tag{100}$$

and Prandtl number is :

$$\mathrm{Pr}_{nf} = \frac{\upsilon_{nf}}{\alpha_{nf}} \tag{101}$$

and then, results :

$$h = \frac{Nuk_{nf}}{d} \tag{102}$$

The temperature and velocity profiles can be viewed post processing. In figure 8 is illustrated one example of visualization the temperature profile in a case study, depending by the boundary conditions imposed.

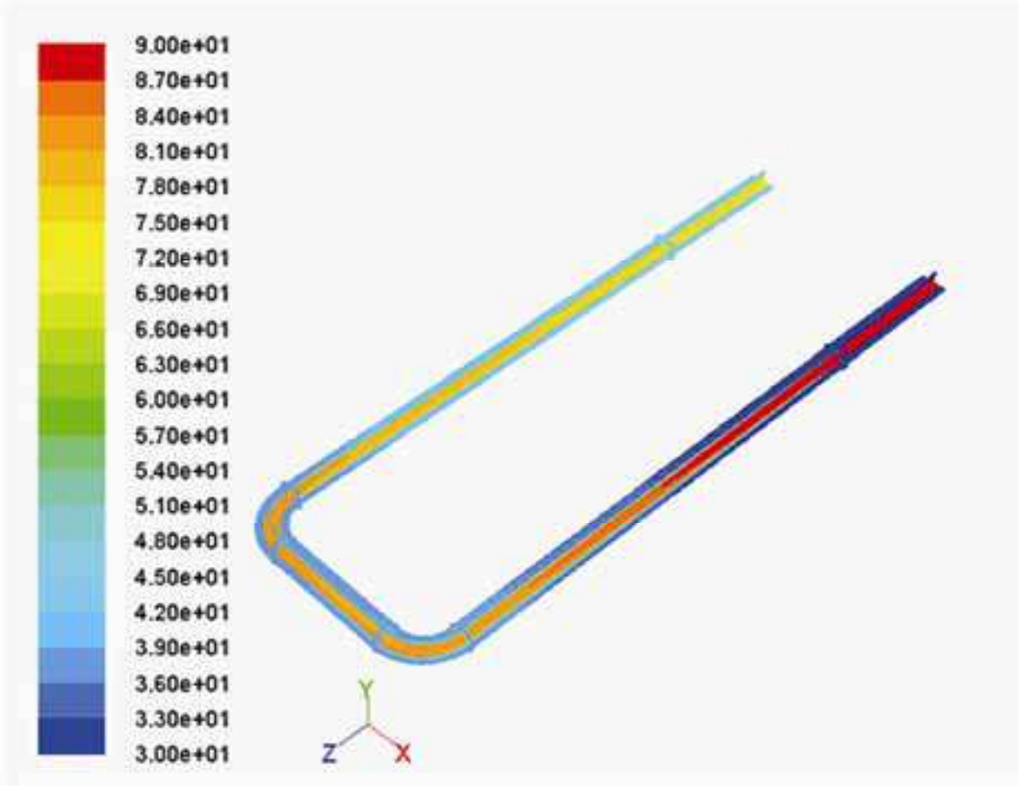

Fig. 8. Temperature profile

Following we analyze the variation of convective heat transfer coefficient in comparison with flow regime, temperature and nanofluids concentrations.
Figures 9-11 highlights the results of values of water and three types of nanofluids used depending on the Reynolds number and the primary agent temperature.

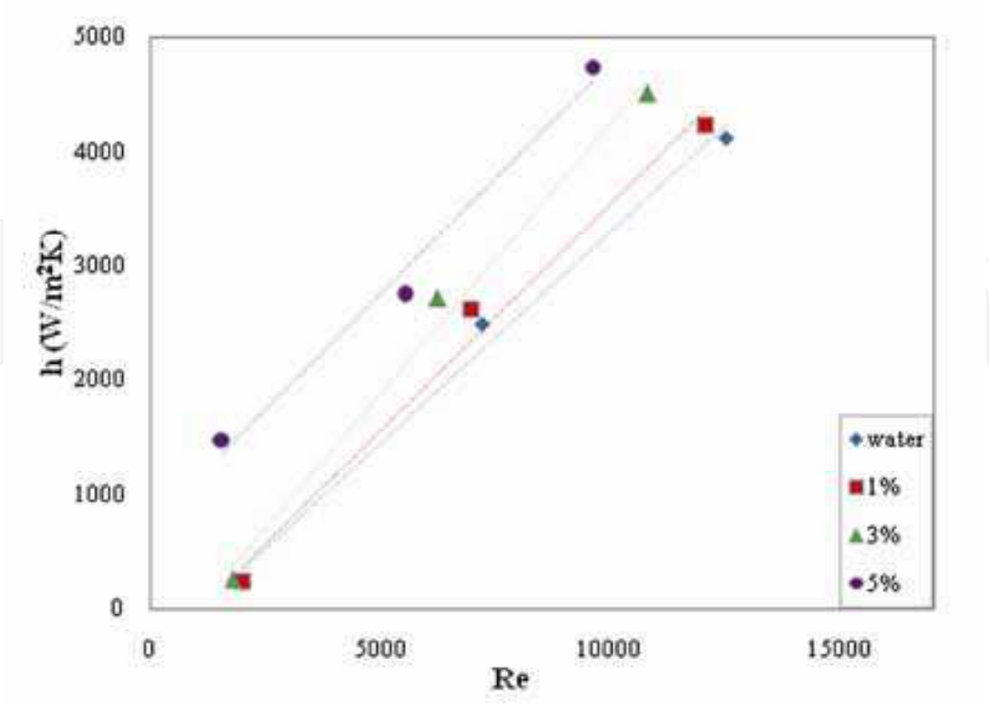

Fig. 9. Variation of convective heat transfer coefficient based on the Reynolds number at the T=60°C

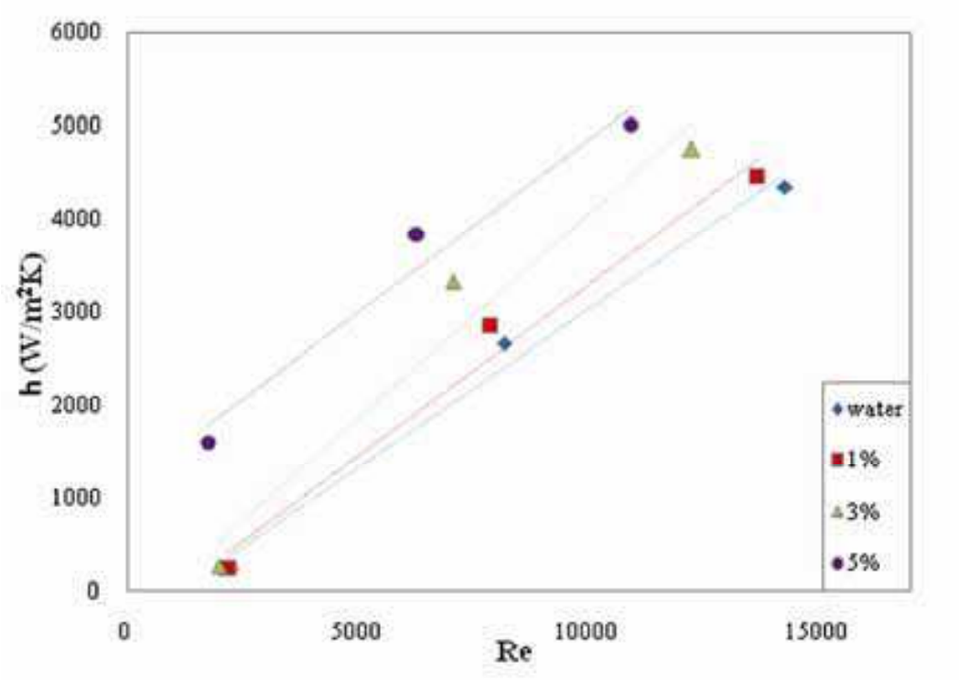

Fig. 10. Variation of convective heat transfer coefficient based on the Reynolds number at the T=70°C

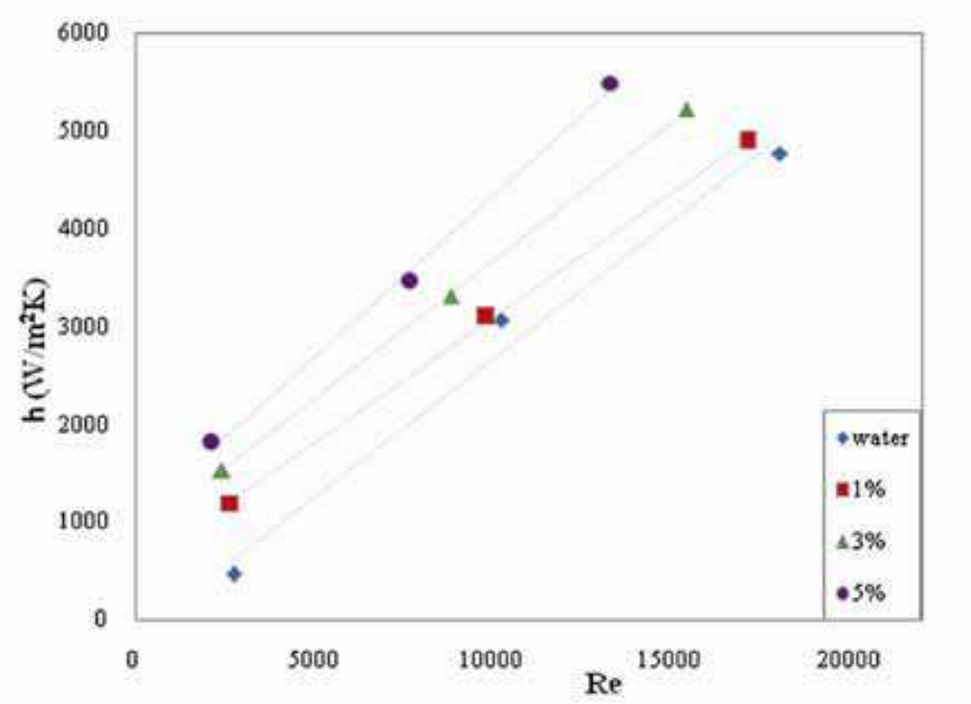

Fig. 11. Variation of convective heat transfer coefficient based on the Reynolds number at the T=90°C

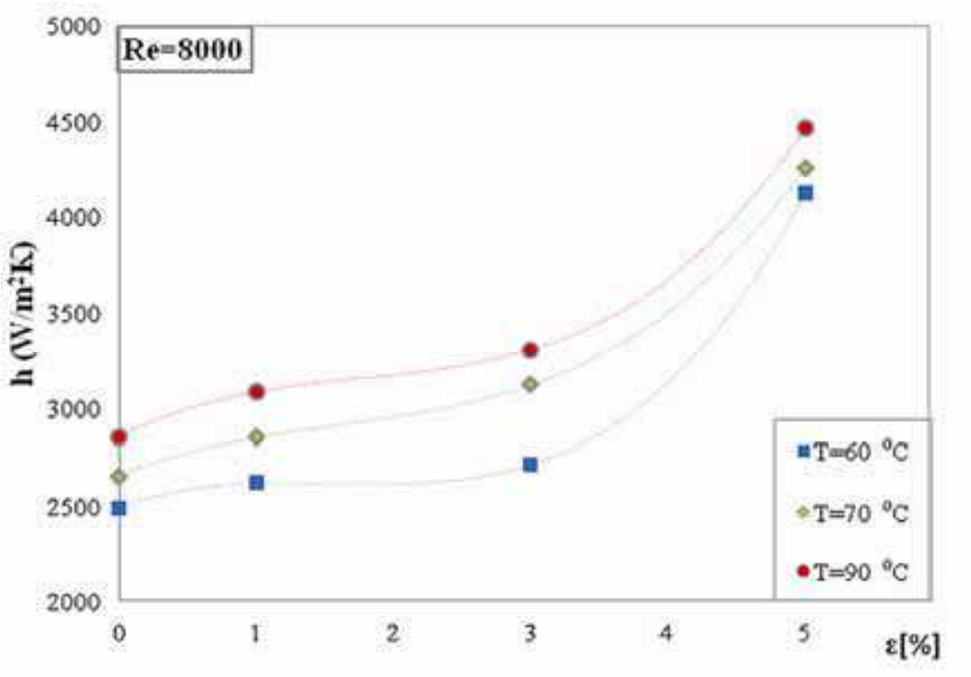

Fig. 12. Variation of convective heat transfer coefficient based on temperature at Reynolds number equal to 8000

It can be seen that the value of convective heat transfer coefficient h for water is about 13% lower than the nanofluids, also parietal heat transfer increases with increasing the primary agent temperature and implicitly with increasing of volume concentration.
In Figure 12 is represented the variation of convective heat transfer coefficient h depending on the volume concentration of particles at imposed temperatures (60, 70 and 90 degree C) for Reynold's number equal to 8000.
We can notice a significant increase of approximately 50% for convective heat transfer coefficient for nanofluid at 5% concentration, compared with water at 90 degree C.

5. The dispersive approximation in the heat transfer processes

In the dispersive approximation of the fractal heat transfer the relation becomes a Korteweg de Vries type equation for the temperature field

$$\frac{\hat{\partial}T}{\partial t}=\frac{\partial T}{\partial t}+\hat{\boldsymbol{V}}\cdot\nabla T+\frac{\sqrt{2}}{3}\mathsf{D}^{3/2}\left(dt\right)^{(3/D_F)-1}\nabla^3 T=0 \tag{103}$$

Separating the real and imaginary parts in Eq.(103), *i.e.*

$$\begin{aligned}&\frac{\partial T}{\partial t}+\boldsymbol{V}\cdot\nabla T+\frac{\sqrt{2}}{3}\mathsf{D}^{3/2}\left(dt\right)^{(3/D_F)-1}\nabla^3 T=0\\&-\boldsymbol{U}\cdot\nabla T=0\end{aligned} \tag{104a,b}$$

and adding them the heat transfer equation is obtained as:

$$\frac{\partial T}{\partial t}+\left(\boldsymbol{V}-\boldsymbol{U}\right)\cdot\nabla T+\frac{\sqrt{2}}{3}\mathsf{D}^{3/2}\left(dt\right)^{(3/D_F)-1}\nabla^3 T=0 \tag{105}$$

From Eq.(104b) we see that at the fractal scale there isn't any thermal convection.
Assuming that $\left|\boldsymbol{V}-\boldsymbol{U}\right|=\sigma T$, with $\sigma=\text{constant}$ (for this assumption see (Agop et al., 2008)), in the one-dimensional case, the equation (52), with the dimensionless parameters

$$\tau=\omega t,\ \xi=kx,\ \phi=\frac{T}{T_0} \tag{106a-c}$$

and the normalizing conditions

$$\frac{\sigma T_0 k}{6\omega}=\frac{\sqrt{2}}{3}\frac{\mathsf{D}^{3/2}\left(dt\right)^{(3/D_F)-1}k^3}{\omega}=1 \tag{107}$$

takes the form:

$$\partial_\tau\phi+6\phi\,\partial_\xi\phi+\partial_{\xi\xi\xi}\phi=0 \tag{108}$$

Through the substitutions

$$w\left(\theta\right)=\phi\left(\tau,\xi\right),\ \theta=\xi-u\tau \tag{109a,b}$$

the Eq.(108), by double integration, becomes

$$\frac{1}{2}w'^2 = F(w) = -\left(w^3 - \frac{u}{2}w^2 - gw - h \right) \tag{110}$$

with g, h two integration constants and u the normalized phase velocity. If $F(w)$ has real roots, the equation (108) has the stationary solution

$$\phi(\xi,\tau,s) = 2a\left(\frac{E(s)}{K(s)} - 1 \right) + 2a \cdot \mathrm{cn}^2\left[\frac{\sqrt{a}}{s}\left(\xi - \frac{u}{2}\tau + \xi_0 \right); s \right] \tag{111}$$

where cn is the Jacobi's elliptic function of s modulus (Bowman, 1953), a is an amplitude, ξ_0 is a constant of integration and

$$K(s) = \int_0^{\pi/2} \left(1 - s^2 \sin^2\varphi\right)^{-1/2} d\varphi,\ E(s) = \int_0^{\pi/2} \left(1 - s^2 \sin^2\varphi\right)^{1/2} d\varphi \tag{112a,b}$$

are the complete elliptic integrals (Bowman, 1953). As a result, the heat transfer is achieved by one-dimensional cnoidal oscillation modes of the temperature field (see Fig.13a). This process is characterized through the normalized wave length (see Fig.13b):

$$\lambda = \frac{2sK(s)}{\sqrt{a}} \tag{113}$$

and normalized phase velocity (see Fig.13c):

$$u = 4a\left[3\frac{E(s)}{K(s)} - 1 - \frac{1}{s^2} \right] \tag{114}$$

In such conjecture, the followings result:

i. the parameter s becomes a measure of the heat transfer. The one-dimensional cnoidal oscillation modes contain as subsequences for $s = 0$ the one-dimensional harmonic waves while for $s \to 0$ the one-dimensional waves packet. These two subsequences describe the heat transfer through the non-quasi-autonomous regime. For $s = 1$, the solution (111) becomes a one-dimensional soliton, while for $s \to 1$ the one-dimensional solitons packet results. These last two subsequences describe the heat transfer through the quasi-autonomous regime;
ii. by eliminating the parameter a from relations (113) and (114), one obtains the relation:

$$\begin{aligned} u\lambda^2 &= A(s) \\ A(s) &= 16\left[3s^2E(s)K(s) - \left(1 - s^2K^2(s)\right) \right] \end{aligned} \tag{115a,b}$$

We observe from Fig.13d that only for $s = 0 \div 0.7$, $A(s) \approx \text{const.}$, and $u\lambda^2 \approx \text{const.}$. According with previous transport regimes, this dispersion relation is valid only for the non-quasi-autonomous regime. For the quasi-autonomous regime it has no signification. Moreover, these two regimes (non-quasi-autonomous and quasi-autonomous) are separated

by the 0.7 experimental structure (Chiatti et al., 1970). We note that the cnoidal oscillation modes can be assimilated to a non-linear Toda lattice (Toda, 1989). In such conjecture, the ballistic thermal phononic transport can be emphasized.

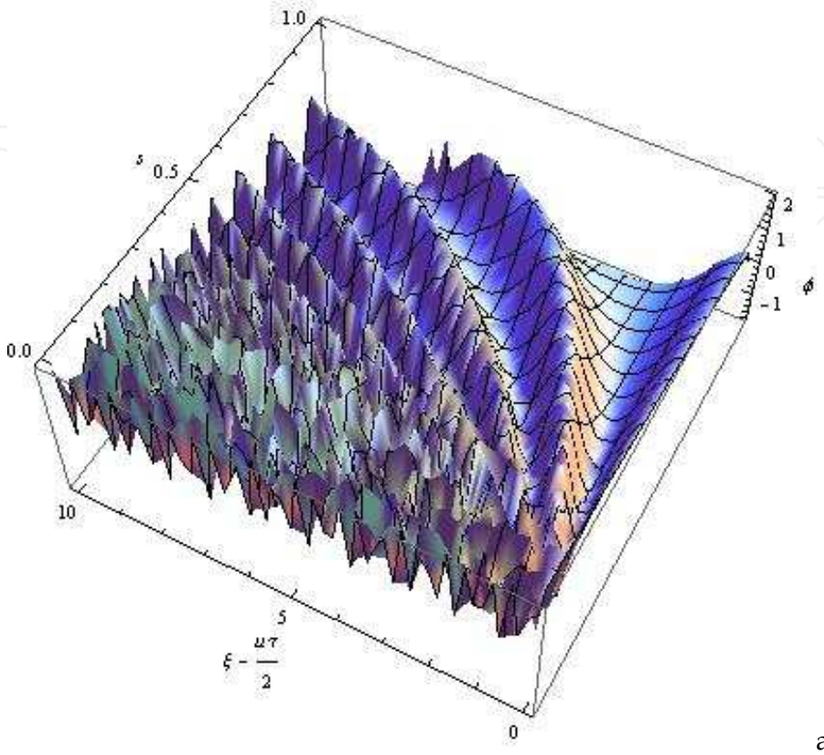

a)

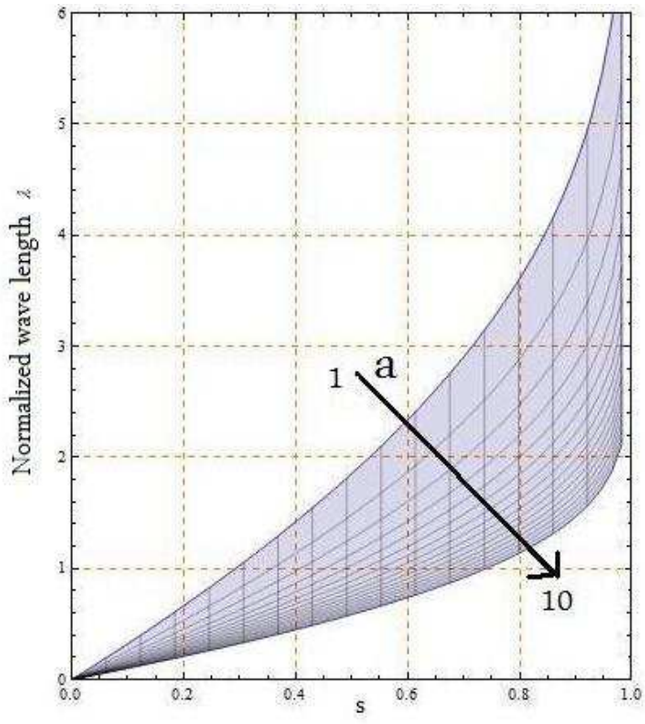

b)

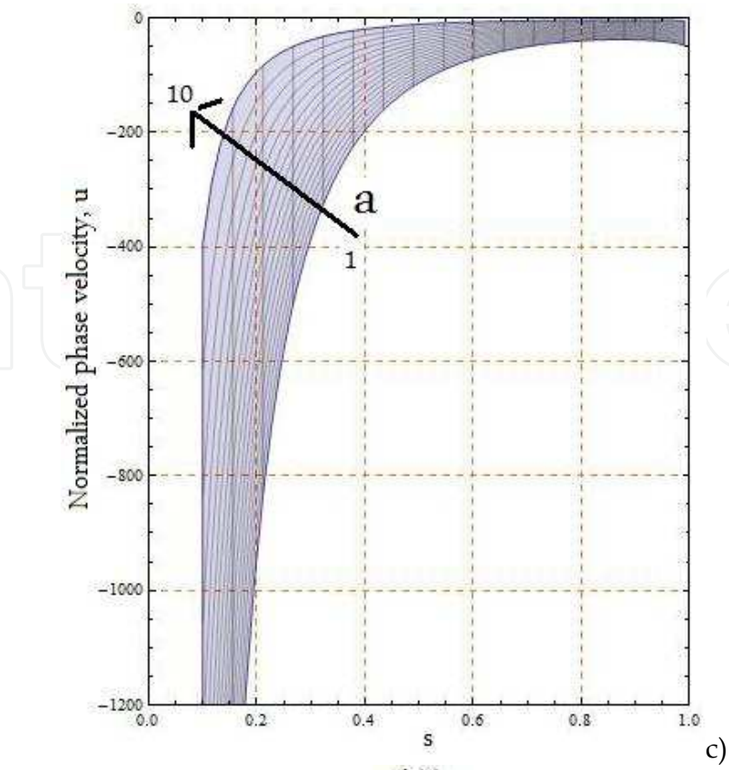

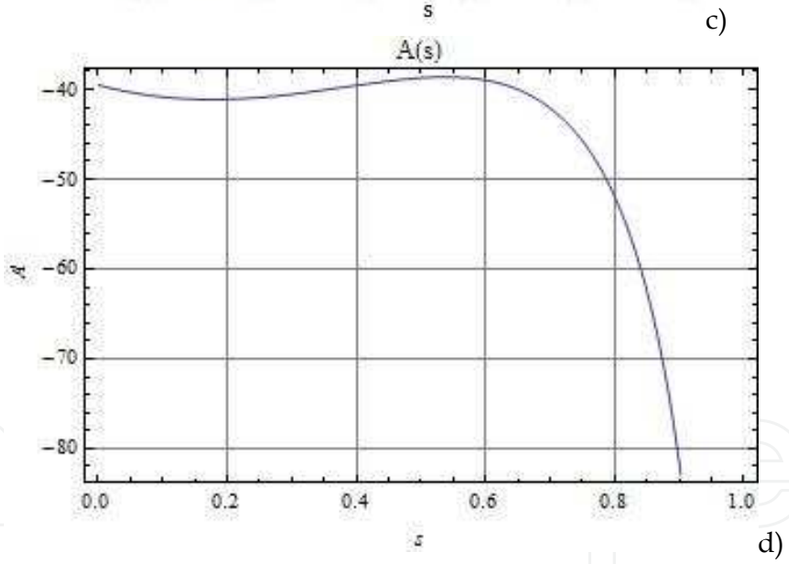

Fig. 13. One-dimensional cnoidal oscillation modes of the temperature field (a) ; normalized wave length (b); normalized phase velocity (c); separation of the thermal flowing regimes (non-quasi-autonomous and quasi-autonomous) by means of the 0.7 experimental structure (Jackson, 1991)

Let us study the influence of fractality on the heat transfer. This can be achieved by the substitutions:

$$w = \frac{u}{4} f^2, \frac{2\theta}{\sqrt{u}} = i\beta \tag{116a,b}$$

and the restriction $h=0$ in Eq.(110). We obtained a Ginzburg-Landau (GL) type equation (Jackson, 1991; Poole et al., 1995):

$$\partial_{\beta\beta} f = f^3 - f \tag{117}$$

The following result:

i. The β coordinate has dynamic significations and the variable f has probabilistic significance;
ii. The general solution of GL equation (Jackson, 1991):

$$f = \sqrt{\frac{2s^2}{1+s^2}}\,\mathrm{sn}\left(\frac{\beta-\beta_0}{\sqrt{1+s^2}};s\right), \beta_0 = \text{const.} \tag{118a,b}$$

where sn is the Jacobi elliptic function of s modulus (Bowman, 1953) (see Fig14), i.e. the fractalisation of the thermal flowing regime, implies the dependence on s of the following parameters:

i. The relative pair breaking time

$$\tau_r = \left(1+s^2\right)K^2(s) \tag{119}$$

ii. The relative concentration

$$n_r = \frac{2}{1+s^2}\left(1-\frac{E(s)}{K(s)}\right) \tag{120}$$

iii. The relative thermal conductivity

$$k_r = 2K(s)\left(K(s)-E(s)\right) \tag{121}$$

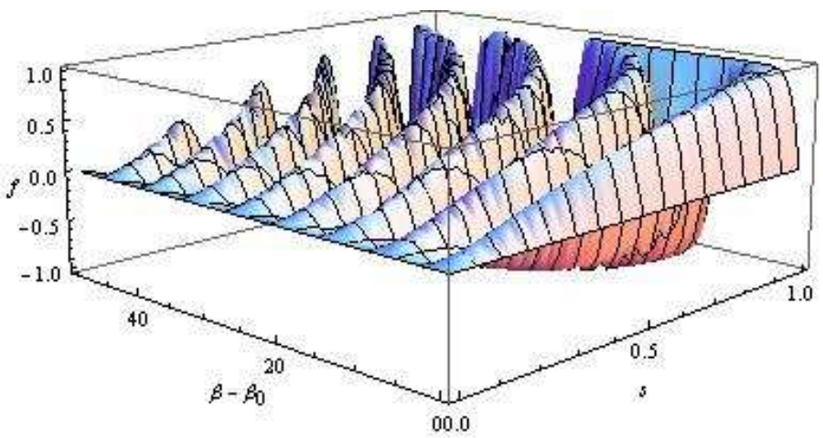

Fig. 14. The fractalisation of the thermal flowing regime is introduced by means of GL equation

These parameters are discontinuous at $s=1$ (see Figs 15a-c), which allows us to say that this singularity can be associated with a phase transition, e.g. from self-structuring to normal state.

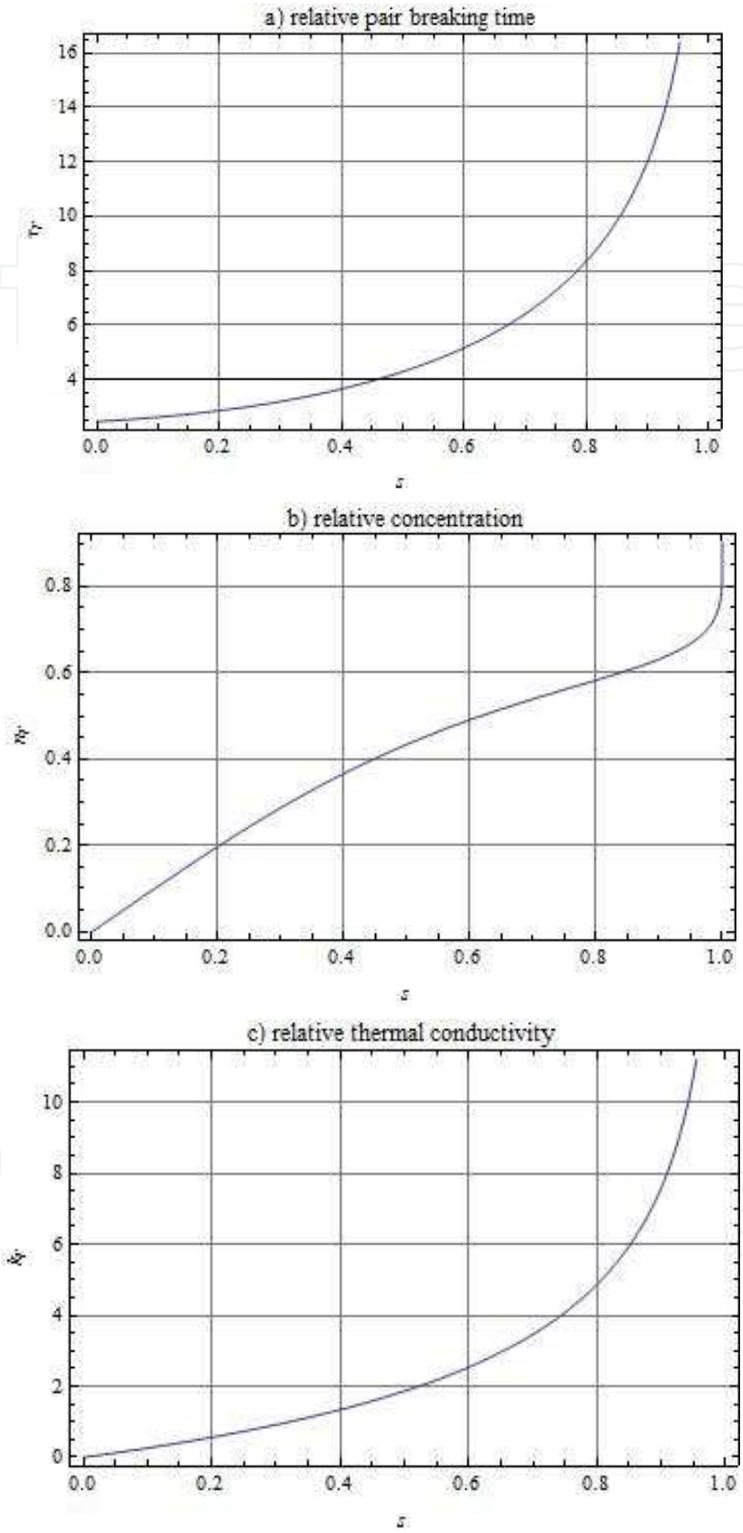

Fig. 15. The dependences on s for: relative pair breaking time τ_r (a); relative concentration n_r (b); relative thermal conductivity k_r (c)

Since the general solution of GL equation is (118a), the self-structuring process is controlled by means of the normalized fractal potential,

$$Q(\beta,s)=-\frac{1}{f}\frac{d^2f}{d\beta^2}=\left(1-f^2\right)=\frac{1-s^2}{1+s^2}+\frac{2s^2}{1+s^2}\mathrm{cn}^2\left(\frac{\beta-\beta_0}{\sqrt{1+s^2}};s\right) \tag{122}$$

also through cnoidal modes. Thus, for $s\to 0$ it results the non-quasi-autonomous regime (of wave packet type),

$$Q(\beta,s\to 0)=\frac{1-s^2}{1+s^2}+\frac{2s^2}{1+s^2}\cos^2\left(\frac{\beta-\beta_0}{\sqrt{1+s^2}};s\right) \tag{123}$$

and for $s\to 1$ the quasi-autonomous regime (of soliton packet type),

$$Q(\beta,s\to 1)=\frac{1-s^2}{1+s^2}+\frac{2s^2}{1+s^2}\mathrm{sech}^2\left(\frac{\beta-\beta_0}{\sqrt{1+s^2}};s\right) \tag{124}$$

For $s=1$ the soliton (118a) is reduced to the fractal kink,

$$f_k(\beta)=\tanh\left(\frac{\beta-\beta_0}{\sqrt{2}}\right) \tag{125}$$

and we can build a field theory with spontaneous symmetry breaking. The fractal kink spontaneously breaks the vacuum symmetry by tunneling and generates pairs of Copper's type (Chaichian&Nelipa, 1984).

iv. The normalized fractal potential (122) take a very simple expression which is proportional with the density of states of the Cooper pairs type. When the density of states of the Cooper pairs type, f^2, becomes zero, the fractal potential takes a finite value, $Q=1$. The fractal fluid is normal (it works in a non-quasi-autonomous regime) and there are no coherent structures (Cooper pairs type) in it. When f^2 becomes 1, the fractal potential is zero, *i.e.* the entire quantity of energy of the fractal fluid is transferred to its coherent structures, *i.e.* to the Cooper pairs type. Then the fractal fluid becomes coherent (it works in a quasi-autonomous regime). Therefore, one can assume that the energy from the fractal fluid can be stocked by transforming all the environment's entities into coherent structures (Cooper pairs type) and then "freezing" them. The coherent fluid acts as an energy accumulator through the fractal potential (122).

6. Conclusions

A new model on the heat transfer processes in nanostructures considering that the heat flow paths take place on fractal curves is obtained. It results:

i. In the dissipative approximation of the heat transfer process, for Peano type heat flow paths and synchronous movements at differentiable and non-differentiable scales, the thermal transfer mechanism is of diffusive type. In such conjecture, numerical solutions in the absence and in the presence of "walls" are obtained.

For a nanofluid, the increasing of the thermal conductivity depends on the ratio of conductivitie (nano-particle/fluid), volume fraction of the nanoparticle and the nanoparticle radius. Moreover, a temperature dependence of the thermal conductivity is olso given.

ii. In the dispersive approximation of the heat transfer process, both at differentiable and non-differentiable scales, the thermal transfer mechanism is given through the cnoidal oscillation modes of the temperature field. Two thermal flow regimes result: one by means of waves and wave packets and the other by means of solitons and soliton packets. These two regimes are separated by the 0.7 experimental "structure".
Since the cnoidal oscillation modes can be assimilated with a non-linear Toda lattice, a ballistic thermal phononic transport can be emphasized.

iii. It result an unique mechanism of thermal transfer in nanostructures in which the usual ones (diffusive type, ballistic phononic type, etc.) can be seen as approximations of the present approach.

iv. For convective type behavior of a complex fluid, numerical studies of a coaxial heat exchanger using nanofluids are presented.

Then single-phase model have been used for prediction of flow field and calculation of heat transfer coefficient. The study present here indicate the thermal performances of a particular nanofluid composed of aluminum oxide (Al_2O_3) particles dispersed in water for various concentrations ranging from 0 to 5 %. Results have shown that heat transfer coefficient clearly increases with an increase in particle concentration.

The results clearly show that the addition of particles in a base fluid produces a great increase in the heat transfer (≈50%). Intensification of heat transfer increases proportionally with increasing of volume concentration of these nanoparticles.

In the present model the values of convective heat transfer coefficient are dependent of flow regime and temperature values. When temperature is higher, the value of this coefficient increases.

7. References

Agop M., Forna N., Casian Botez I., Bejenariu C., J. (2008), New Theoretical Approach of the Physical Processes in Nanostructures, *Comput. Theor. Nanos*, Vol. 5, No. 4, pp.483-489

Akbarinia A., Behzadmehr A. (2007), Numerical study of laminar mixed convection of ananofluid in horizontal curved tube, *Applied Thermal Science*, Vol. 27, No. 8-9, pp. 1327–1337

Albeverio S., Hoegh-Krohn R. (1974), A remark on the connection between stochastic mechanics and the heat equation, *Journal of Mathematical Physics*, Vol 15., No 10, pp. 1745-1747

Agop M., Paun V., Harabagiu A. (2008), El Naschie's $\varepsilon(\infty)$ theory and effects of nanoparticle clustering on the heat transport in nanofluids, *Chaos Solitons & Fractals*, Vol. 37, No. 5, pp. 1269-1278

Bianco V., Chiacchio F., Manca O., Nardini (2009), Numerical investigation of nanofluids forced convection in circular tube, *Applied Thermal Engineering*, Vol. 29, No. 17-18, pp. 3632-3642

Bowman F. (1953), *Introduction to Elliptic Functions with Applications*, English Universities Press, London

Chen G. (2000), Particularities of Heat Conduction in Nanostructures, *J.Nanopart. Res.*, Vol. 2, No. 2, pp. 199-204

Casian Botez I., Agop M., Nica P., Paun V., Munceleanu G.V. (2010), Conductive and Convective Types Behaviors at Nano-Time Scales, *J. Comput. Theor. Nanos*., Vol. 7, No. 11, pp. 2271-1180

Chiroiu V., Stiuca P., Munteanu L., Danescu S. (2005), *Introduction in nanomechanics*, Roumanian Academy Publishing House, Bucuresti,

Chiatti O., Nicholls J.T., Proskuryakov Y.Y., Lumpkin N., Farrer I., Ritchie D.A. (2006), Quantum thermal conductance of electrons in a one-dimensional wire, *Phys. Rev. Lett.*, Vol. 97, No. 5

Chaichian M., Nelipa N.F (1984), *Introduction to Gauge Field Theories. Texts and Monographs in Physics*, Springer-Verlag Berlin-Heidelberg-New York-Tokyo

Ferry D.K., Goodnick S.M. (1997), *Transport in Naostructures*, Cambridge University Press, Cambridge, U.K.

Fard M. H., Esfahany M. N. , Talaie M.R. (2009 in press), Numerical study of convective heat transfer of nanofluids in a circular tube two-phase model versus single-phase model, *International Communications in Heat and Mass Transfer*

Hemanth Kumar D., Patel H.E., Rajeev Kumar V.R., Sundararajan Pradeep T., Das S.K. (2004), Model for Heat Conduction in Nanofluids, *Phys. Rev. Lett.*, Vol. 93, No. 14, p. 144301

Harvey R.J. (1966), Navier-Stokes Analog of Quantum Mechanics, *Physical Review*, Vol 152, No 4, p 1115

Jang S.P., Choi S.U. (2004), Role of Brownian motion in the enhaced thermal conductivity of nanofluids, *Applied Physics Letters*, Vol. 84, No. 21, p. 4316

Jackson E. A. (1991), *Perspectives in Nonlinear Dynamics*, Vol. 1, 2, Cambridge University Press, Cambridge, U. K.

Keblinski P., Phillpot S.R., Choi S.U.S., Eastman J.A. (2002), Mechanisms of heat flow in suspensions of nano-sized particles (nanofluids), *Int. J. Heat and Mass. Transfer*, Vol. 45, No. 4, pp. 855-863

Kumar D. H., Patel H. E., Rajeev Kumar V.R., Sundararajan T., Pradeep T., Das S.K. (2004), Model for Heat Conduction in Nanofluids, *Physical Review Letters*, Vol. 93, No. 14, p. 144301

Landau L., Lifshitz E. (1987), *Fluid Mechanics*, Butterworth-Heinemann, Oxford

Mandelbrot B. (1982), *The Fractal Geometry of Nature*, Freeman, San Francisco, U.S.A.

Maiga S.E.B., Palm S.J., et al. (2005), Heat transfer enhancement by using nanofluids in forced convection flows, *International Journal of Heat and Fluid Flow*, Vol. 26, No.4, pp. 530–546

Maiga S.E.B., Nguyen C.T., Galanis N., Roy G. (2004), Heat transfer behavior of nanofluids in a uniformly heated tube, *Superlattices and Microstructures*, Vol. 35, No. 3-6,pp. 543–557

Maiga S.E.B, Nguyen C.T. (2006), Heat transfer enchancement in turbulent tube flow using Al2O3 nanoparticles suspension, *International Journal of Numerical Methods for Heat and Fluid Flow*, Vol 16, No 3, pp. 275 - 292

Nottale L. (1992), *Fractal Space-Time and Microphysics: Towards a Theory of Scale Relativity*, Word Scientific, Singapore

Nottale L., Ch. Auffray (2008), Scale relativity theory and integrative systems biology: 2 Macroscopic quantum-type mechanics, *Prog. Biophys. Mol. Bio.*, Vol. 97, No. 1, pp. 115-157

Nottale L. (2008), *Scale relativity and fractal space-time: theory and applications*, First International Conference on the Evolution and Development of the Universe, Paris

Notalle L. (2007), Scale Relativity: A Fractal Matrix for Organization in Nature, *Electronic Journal of Theoretical Physics*, Vol. 4, No.16 (III), pp. 15-102

Nikitov A. and Ouvanov V. (1974), *Élémentes de la Théorie des Functions Spéciales*, Mir, Moscow

Nguyen C. T., Roy G., Lajoie P.R. (2005), *Refroidissement des microprocesseurs à haute performance en utilisant des nano fluides*, Congrès Français de Thermique, SFT Reims

HE Patel, SK Das, T. Sundararajan, AS Nair, B. George, T. Pradeep (2003), Thermal conductivities of naked and monolayer protected metal nanoparticle based nanofluids: Manifestation of anomalous enhancement and chemical effects, *Appl.Phys.Lett.*,Vol. 83, No.14, p. 2931

Patankar S.V. (1980), *Numerical heat transfer and fluid flow*, Hemisphere Publishing Corporation, Taylor and Francis Group, New York

Pak, B. C. et Cho, Y. I. (1998), Hydrodynamic and Heat Transfer Study of Dispersed Fluids with Submicron Metallic Oxide Particles, *Experimental Heat Transfer*, Vol. 11, No. 2, pp. 151-170

Poole Ch.P. Jr., Farach H.A., Creswick R.J. (1995), *Textbook of Superconductivity*, Academic Press, San Diego

Prasher R. (2005), Thermal Conductivity of Nanoscale Colloidal Solutions (nanofluids), *Physical Review Letters*, Vol. 94, No.2, p. 025901

Rohsenow HW.M., Hartnett J.P., Cho Y.I. (1998), *Handbook of Heat Transfer*, McGraw Hill, U.S.A.

Toda M. (1981), *Theory of Nonlinear Lattices*, Springer Series in Solid-State Sciences 20, Springer-Verlag

Vizureanu P., Agop M. (2007), A Theoretical Approach of the Heat Transfer in Nanofluids, *Materials Transactions*, Vol. 48, No. 11, pp. 3021-3023

Vasu V., Rama K.K., Kumar A.C.S. (Article in press), Empirical correlations to predict thermophysical and heat transfer characteristics of nanofluids, *Thermal Science Journal*, Vol. 12, No. 3

Wang J.-S., Wang J. and Lii J.T. (2008), Quantum thermal transport in nanostructures, *Eur. Phys. Jour. B*, Vol 62, No. 4, pp. 381-404

Wang X., Xu X., J. (1999), Thermal Conductivity of Nanoparticle-Fluid Mixture, *Jour. Thermophys. And Heat Transfer*, Vol. 13, No. 4, pp. 474-480

Zhang Z. (2007), *Nano-Microscale Heat Transfer*, McGraw Hill, U.S.A.

Zienkievicz O.C., Taylor R.L. (1991), *The Finite Element Method*, McGraw-Hill, New York, U.S.A.

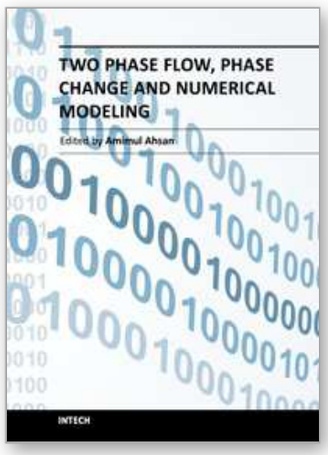

Two Phase Flow, Phase Change and Numerical Modeling
Edited by Dr. Amimul Ahsan

ISBN 978-953-307-584-6
Hard cover, 584 pages
Publisher InTech
Published online 26, September, 2011
Published in print edition September, 2011

The heat transfer and analysis on laser beam, evaporator coils, shell-and-tube condenser, two phase flow, nanofluids, complex fluids, and on phase change are significant issues in a design of wide range of industrial processes and devices. This book includes 25 advanced and revised contributions, and it covers mainly (1) numerical modeling of heat transfer, (2) two phase flow, (3) nanofluids, and (4) phase change. The first section introduces numerical modeling of heat transfer on particles in binary gas-solid fluidization bed, solidification phenomena, thermal approaches to laser damage, and temperature and velocity distribution. The second section covers density wave instability phenomena, gas and spray-water quenching, spray cooling, wettability effect, liquid film thickness, and thermosyphon loop. The third section includes nanofluids for heat transfer, nanofluids in minichannels, potential and engineering strategies on nanofluids, and heat transfer at nanoscale. The forth section presents time-dependent melting and deformation processes of phase change material (PCM), thermal energy storage tanks using PCM, phase change in deep CO2 injector, and thermal storage device of solar hot water system. The advanced idea and information described here will be fruitful for the readers to find a sustainable solution in an industrialized society.

How to reference
In order to correctly reference this scholarly work, feel free to copy and paste the following:

Maricel Agop, Irinel Casian Botez, Luciu Razvan Silviu and Manuela Girtu (2011). Heat Transfer in Nanostructures Using the Fractal Approximation of Motion, Two Phase Flow, Phase Change and Numerical Modeling, Dr. Amimul Ahsan (Ed.), ISBN: 978-953-307-584-6, InTech, Available from: http://www.intechopen.com/books/two-phase-flow-phase-change-and-numerical-modeling/heat-transfer-in-nanostructures-using-the-fractal-approximation-of-motion

INTECH
open science | open minds

InTech Europe
University Campus STeP Ri
Slavka Krautzeka 83/A
51000 Rijeka, Croatia
Phone: +385 (51) 770 447
Fax: +385 (51) 686 166
www.intechopen.com

InTech China
Unit 405, Office Block, Hotel Equatorial Shanghai
No.65, Yan An Road (West), Shanghai, 200040, China
中国上海市延安西路65号上海国际贵都大饭店办公楼405单元
Phone: +86-21-62489820
Fax: +86-21-62489821

IntechOpen